International Journal of Bifurcation and Chaos, Vol. 15, No. 4 (2005) 1285–1328

GLOBAL BIFURCATIONS OF CLOSED INVARIANT CURVES IN TWO-DIMENSIONAL MAPS: A COMPUTER ASSISTED STUDY

ANNA AGLIARI
Istituto di Econometria e Matematica AEFA,
Catholic University of Milano, Italy
anna.agliari@unicatt.it

GIAN-ITALO BISCHI
Istituto di Scienze Economiche, University of Urbino, Italy
bischi@econ.uniurb.it

ROBERTO DIECI
Dipartimento di Matematica per le Scienze Economiche e Sociali,
University of Bologna, Italy
rdieci@rimini.unibo.it

LAURA GARDINI*
Istituto di Scienze Economiche, University of Urbino, Italy
gardini@econ.uniurb.it

Received January 5, 2004; Revised February 4, 2004

In this paper we describe some sequences of global bifurcations involving attracting and repelling closed invariant curves of two-dimensional maps that have a fixed point which may lose stability both via a supercritical Neimark bifurcation and a supercritical pitchfork or flip bifurcation. These bifurcations, characterized by the creation of heteroclinic and homoclinic connections or homoclinic tangles, are first described through qualitative phase diagrams and then by several numerical examples. Similar bifurcation phenomena can also be observed when the parameters in a two-dimensional parameter plane cross through many overlapping Arnold's tongues.

Keywords: Discrete dynamical systems; invariant curves; global bifurcations; homoclinic tangles; heteroclinic connections.

1. Introduction

Several studies have been devoted to the supercritical Neimark–Hopf bifurcation of fixed points in two-dimensional maps. In particular, a typical and well-known structure of the bifurcation diagram, in a two-dimensional parameter plane, is given by the so-called "Arnold's tongues" issuing from a Neimark–Hopf bifurcation curve. Such tongues do not overlap as far as the parameters are close to the bifurcation curve, while they may overlap when the parameters are taken far enough from the bifurcation curve, denoting an increase of nonlinearity. Inside a tongue, associated with a rotation number p/q, a periodic orbit of period q exists such that the iterations visit all the periodic points every p turns around the fixed point (on this we refer

*Author for correspondence.

to some classical texts, e.g. [Gumowski & Mira, 1980; Guckenheimer & Holmes, 1985; Mira, 1987; Wiggins, 1988; Bai-Lin, 1989; Kuznetsov, 1998]. Other properties of the Arnold tongues have been investigated by several authors, see e.g. [Aaronson *et al.*, 1982; Frouzakis *et al.*, 1991, 1997; Maistrenko *et al.*, 1995; Maistrenko *et al.*, 2003; Sushko *et al.*, 2003], to cite a few. In particular, it is well known that the boundaries of a p/q tongue are saddle-node bifurcation curves of a cycle of period q, and inside the tongue we generally have an attracting closed invariant set formed by a saddle-node connection, that is, the unstable set of the saddle q-cycle reaches the node q-cycle thus forming a closed attracting curve. This is called an *heteroclinic loop*. Similar closed invariant curves, but repelling, are associated with a subcritical Neimark bifurcation. In this case, the cycles involved are a saddle and a repelling node, and the repelling closed invariant curve is made up of the stable set of the saddle cycle, issuing from the repelling node, so that it is again an heteroclinic loop. It is worth noting that closed invariant curves may also be associated with saddle and focus cycles. The difference with respect to the saddle-node connection only concerns the topology of the closed invariant curve. In fact, a closed invariant curve formed by a saddle-node connection (unstable set of the saddle if attracting, stable set of the saddle if repelling) is homeomorphic to a circle, whereas a closed invariant curve made up of a saddle-focus connection (unstable set of the saddle if attracting, stable set of the saddle if repelling) is not homeomorphic to a circle (due to the infinite spiraling of the manifolds around the focus).

In a discrete dynamical system, i.e. an iterated map, the global bifurcations involving closed invariant curves have been less investigated, and several open problems are still present, as remarked in [Kuznetsov, 1998]. The saddle-node bifurcations of closed invariant curves (given by the merging of two closed invariant curves, one attracting and one repelling, followed by their disappearance, or their creation if the movement of the parameters is reversed), quite common in continuous flows, are instead exceptions when we deal with two-dimensional maps.

The main purpose of this paper is to show some mechanisms associated with the appearance and disappearance of closed invariant curves (attracting or repelling). We shall see that a mechanism, that may be considered as typical in some classes of maps, is associated with a saddle-connection, also called *homoclinic loop* defined as a closed invariant curve formed by the merging of a branch of stable set of a periodic point of a saddle cycle with the unstable branch of another periodic point of the same saddle, thus forming a closed connection among the periodic points of the saddle. This is a structurally unstable situation, which causes a bifurcation between two qualitatively different dynamic behaviors. As this kind of bifurcation cannot be predicted by a local investigation, it can be classified as a *global bifurcation*. In particular, the unstable branch of the saddle involved in the bifurcation exhibits different dynamic behaviors before and after the bifurcation, because it reaches a different attracting set. A similar property holds for the stable branch of the saddle involved in the bifurcation: before and after the bifurcation the preimages of the local stable set come from different invariant repelling sets. Such homoclinic loops of saddle are known to occur in the resonant cases of the Neimark-bifurcation (see [Kuznetsov, 1998; Gicquel, 1996]), and recently they have been observed in some families of maps in relation with a subcritical Neimark bifurcation (see [Agliari *et al.*, 2003]). However, we shall see that its occurrence is quite common also far from the Neimark bifurcation, and is related with several bifurcations of closed invariant curves. As we shall see in the examples shown in this paper, when dealing with maps this structurally unstable situation is often replaced by the following sequence of bifurcations: first, a cyclical heteroclinic tangency (or homoclinic tangent bifurcation of nonsimple type, as we shall see in the next section), followed by a parameter range of transverse crossing between the stable and unstable sets of the saddle cycle, that gives rise to cyclical heteroclinic points (or cyclical homoclinic connections), followed by a second cyclical heteroclinic or homoclinic tangency. In other words, the simple homoclinic loop of a saddle is more easily observed in continuous flows, whereas for maps it is generally replaced by a range of parameters that give rise to an homoclinic tangle of the saddle (and related complex dynamics).

The paper is organized as follows. In Sec. 2, we give a qualitative description of the bifurcations which lead to the appearance of closed invariant curves, attracting and repelling, and their further qualitative changes. In Sec. 3, these sequences of bifurcations are shown through numerical explorations by using a family of symmetric maps. An even more rich sequence of bifurcations is shown

in Sec. 4, by using a family of nonsymmetric maps. Finally, in Sec. 5 we consider a third family of maps, given by polynomial maps with a cubic nonlinearity, in order to stress that the bifurcations qualitatively described in Sec. 2 are commonly observed in different kinds of two-dimensional maps.

2. Qualitative Description of the Bifurcations

Let us consider a two-dimensional map T with a fixed point O (that we shall call "basic fixed point" in the following) which is stable inside a given region of the space of the parameters of the map, and can lose stability via a supercritical Neimark bifurcation, as well as a supercritical pitchfork bifurcation or a supercritical flip bifurcation. In other words, we assume that the local stability analysis of the basic fixed point reveals that its stability region is bounded by bifurcation surfaces whose projection in a two-dimensional subspace of the space of the parameters gives one of the situations (or both) represented in Fig. 1, where **P** represents a supercritical pitchfork bifurcation curve, **N** a supercritical Neimark bifurcation curve and **F** a supercritical flip bifurcation curve.

If the parameters are outside the stability region and close to the pitchfork bifurcation curve **P**, then the basic fixed point O is a saddle and two stable fixed points, say Q_1 and Q_2, exist. Instead, if the parameters are beyond the Neimark bifurcation curve **N**, then the basic fixed point O is a repelling focus and a closed invariant attracting curve exists around it. Thus, if we vary the parameters following a bifurcation path like the one indicated in Fig. 1(a), the dynamic scenario must change from the former situation to the latter one, and some global bifurcation must occur leading to the creation of the closed invariant curve. Moreover, the two stable fixed points Q_i must become unstable and merge with the basic fixed point through another bifurcation, occurring when crossing the curve **P** outside of the stability region, where two repelling nodes merge into a saddle, thus disappearing and leaving a repelling node alone. However, also the stable fixed points Q_i are expected to become focuses while moving along that bifurcation path, and become repelling focuses via a subcritical Neimark bifurcation, after which they will become repelling nodes before merging with O. Hence, in this case the appearance of the two repelling closed invariant curves involved in a subcritical Neimark bifurcation of Q_i must be explained. Indeed, we shall see that this is typically associated with the homoclinic bifurcations (or homoclinic tangles) of the basic fixed point.

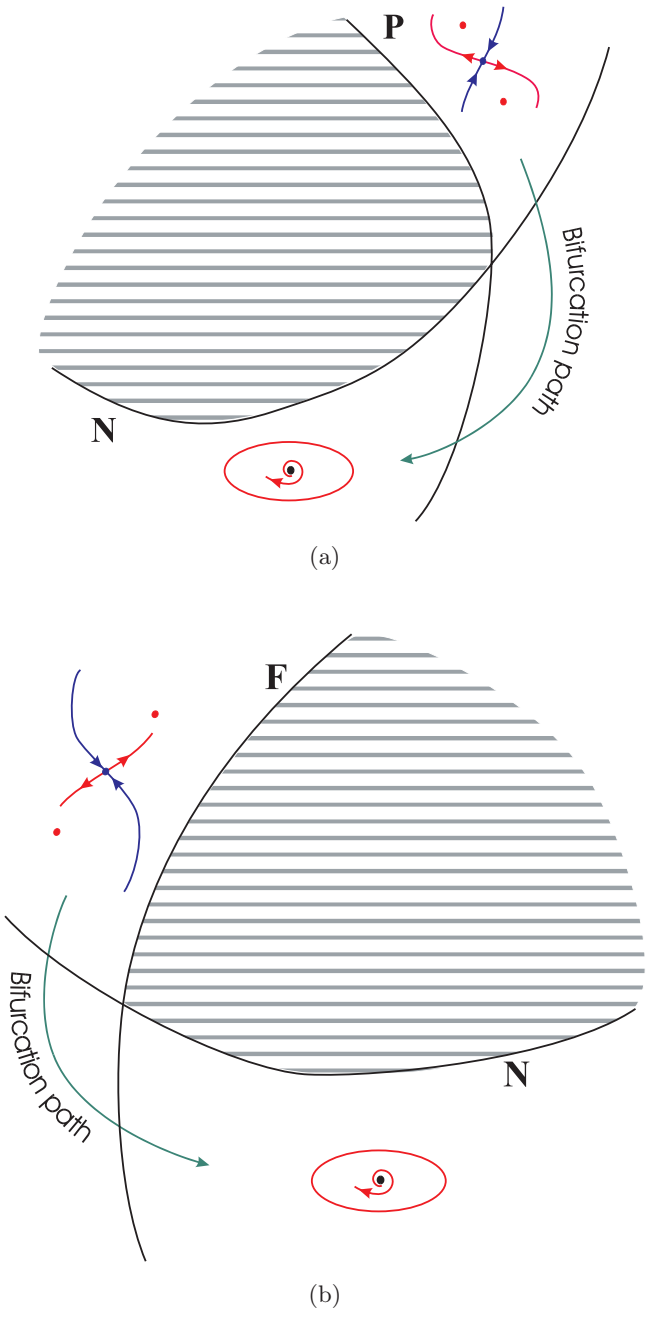

Fig. 1. Qualitative representation, in a two-dimensional subspace of the space of the parameters, of two hypothetical stability regions of basic fixed point (the shaded area). (a) The stability region is bounded by a supercritical Neimark bifurcation curve, denoted by **N**, and a supercritical pitchfork bifurcation curve, denoted by **P**; (b) The stability region is bounded by a supercritical Neimark bifurcation curve and a supercritical flip bifurcation curve **F**.

Similar arguments apply to the case shown in Fig. 1(b), where, again, on one side the stability region is bounded by a supercritical Neimark bifurcation curve, whereas on the other side it is bounded by a supercritical flip bifurcation curve. In this case, if the parameters are outside the stability region and close to the flip bifurcation curve **F**, then the basic fixed point O is a saddle and an attracting cycle of period two exists, say $C_2 = \{Q_1, Q_2\}$. Thus if we vary the parameters from this region to the region close to the curve **N**, following a bifurcation path similar to the one shown in Fig. 1(b), also in this case we should explain the occurrence of some global bifurcations leading to the appearance of the closed invariant curve and the disappearance of the stable cycle. However, if we consider the second iterate of the map, i.e. $T^2 = T \circ T$, instead of T, we are exactly in the same situation described above. In fact, a flip bifurcation of T corresponds to a pitchfork bifurcation of T^2, and the stable periodic points of the cycle C_2 correspond to stable fixed points of the map T^2. This implies that the same global bifurcations are to be expected in the two cases, involving the two periodic points of C_2 instead of the two fixed points previously considered. So, in the following we shall focus our attention on the description of the bifurcations which are expected to occur as we vary the parameters along the bifurcation path indicated in Fig. 1(a), and the same results will also hold along the bifurcation path of Fig. 1(b), with obvious changes.

Before starting the qualitative description of these global bifurcations, let us remind that the dynamics of the restriction of a map to a closed invariant curve (attracting or repelling) is either quasiperiodic (i.e. the limit set of any trajectory on the closed invariant curve is the curve itself), or periodic (i.e. the curve is formed by a saddle-node or saddle-focus connection, as explained in Sec. 1. However, generally the dynamics on the closed curve is periodic, but of very high period, so that it is numerically indistinguishable from a quasiperiodic one.

2.1. *Creation of two closed invariant curves, one attracting and one repelling*

We now start a qualitative description of the sequence of bifurcations that are expected to occur as the parameters of a two-dimensional map are varied along a path like the one represented in Fig. 1(a). As explained above, the fixed points Q_i from attracting nodes become attracting focuses, and then they become repelling focuses via subcritical Neimark bifurcations. Thus we have to explain the creation of the two repelling and disjoint closed invariant curves, which are involved in the subcritical Neimark bifurcations. They constitute the basin boundary of the immediate basin of attraction of the fixed points Q_i. This dynamic situation is generally reached via two distinct global bifurcations: a first one which gives a wide repelling closed invariant curve $\tilde{\Gamma}$, inside which all the three fixed points are located, then this repelling closed invariant curve splits into two disjoint repelling closed invariant curves, each one around a stable fixed point Q_i via a homoclinic bifurcation of the saddle O. Let us first describe the appearance of $\tilde{\Gamma}$. This is associated with a couple of cycles say of period q, born by a saddle-node bifurcation, whose periodic points are located around the three fixed points O and Q_i. This situation is qualitatively described in Fig. 2(a), where for simplicity we have used rotation number $p/q = 4$, with period $q = 4$ and $p = 1$. A similar situation is represented in the qualitative Fig. 2(d), where the stable node of period 4 is replaced by a stable focus with the same period. In these situations, one branch of the unstable set of the saddle tends to the stable cycle, while the other branch of the saddle goes towards the fixed points, as qualitatively shown in the Figs. 2(a) and 2(d). At the bifurcation, the unstable branches $\bigcup \alpha_{1,i}$ and the stable ones $\bigcup \omega_{1,i}$, $i = 1, 2, \ldots, q$, merge in a homoclinic loop, as shown in Figs. 2(b) and 2(e), thus creating a closed invariant curve. After the bifurcation, two closed invariant curves exist [Figs. 2(c) and 2(f)]: one repelling, $\tilde{\Gamma}$, and one attracting, Γ. The latter is the heteroclinic loop made up of the unstable set of the saddle cycle that reaches the attracting cycle, node or focus (see Figs. 2(c) and 2(d), respectively).

2.2. *From one repelling closed invariant curve to two disjoint ones*

The repelling closed invariant curve $\tilde{\Gamma}$ surrounds the two stable fixed points Q_i and the saddle O. The stable set of O, $W^S(O)$, formed by the union of the preimages of any rank of the local stable set, turns around infinitely many times approaching the repelling curve $\tilde{\Gamma}$, as qualitatively shown in Fig. 3(a). $W^S(O)$ constitutes the boundary

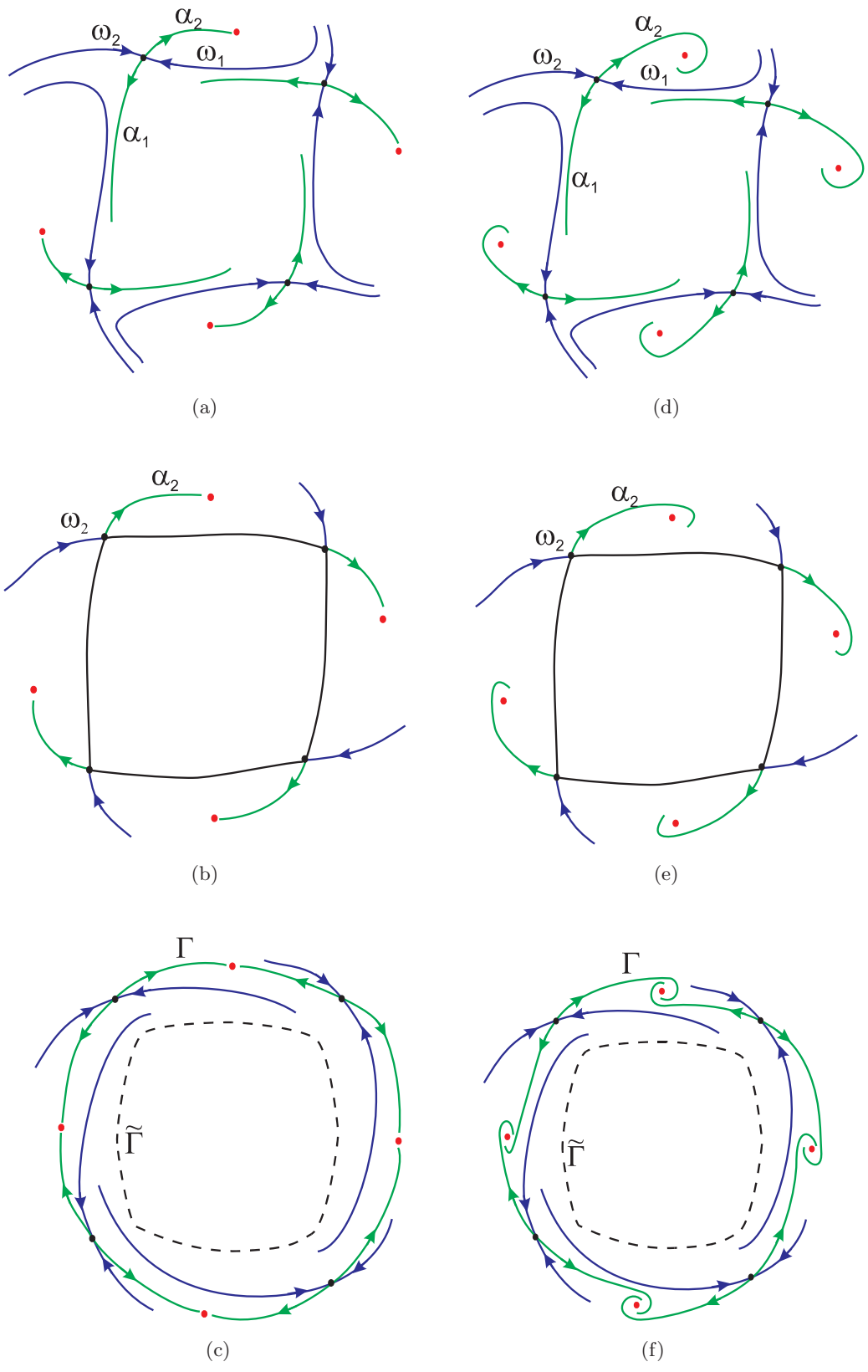

Fig. 2. Qualitative representation of a sequence of global bifurcations leading to the creation of two closed invariant curves, one attracting (Γ) and one repelling ($\tilde{\Gamma}$). In the sequence (a)–(c) a saddle-cycle and a stable node-cycle of the same period are considered, whereas in the sequence (d)–(f) the same bifurcations are described for a saddle-cycle and a stable focus-cycle. The blue curves represent the stable set of the saddle, whose two branches are labeled by ω_1 and ω_2, and the green curves represent the unstable set of the saddle, whose two branches are labeled by α_1 and α_2.

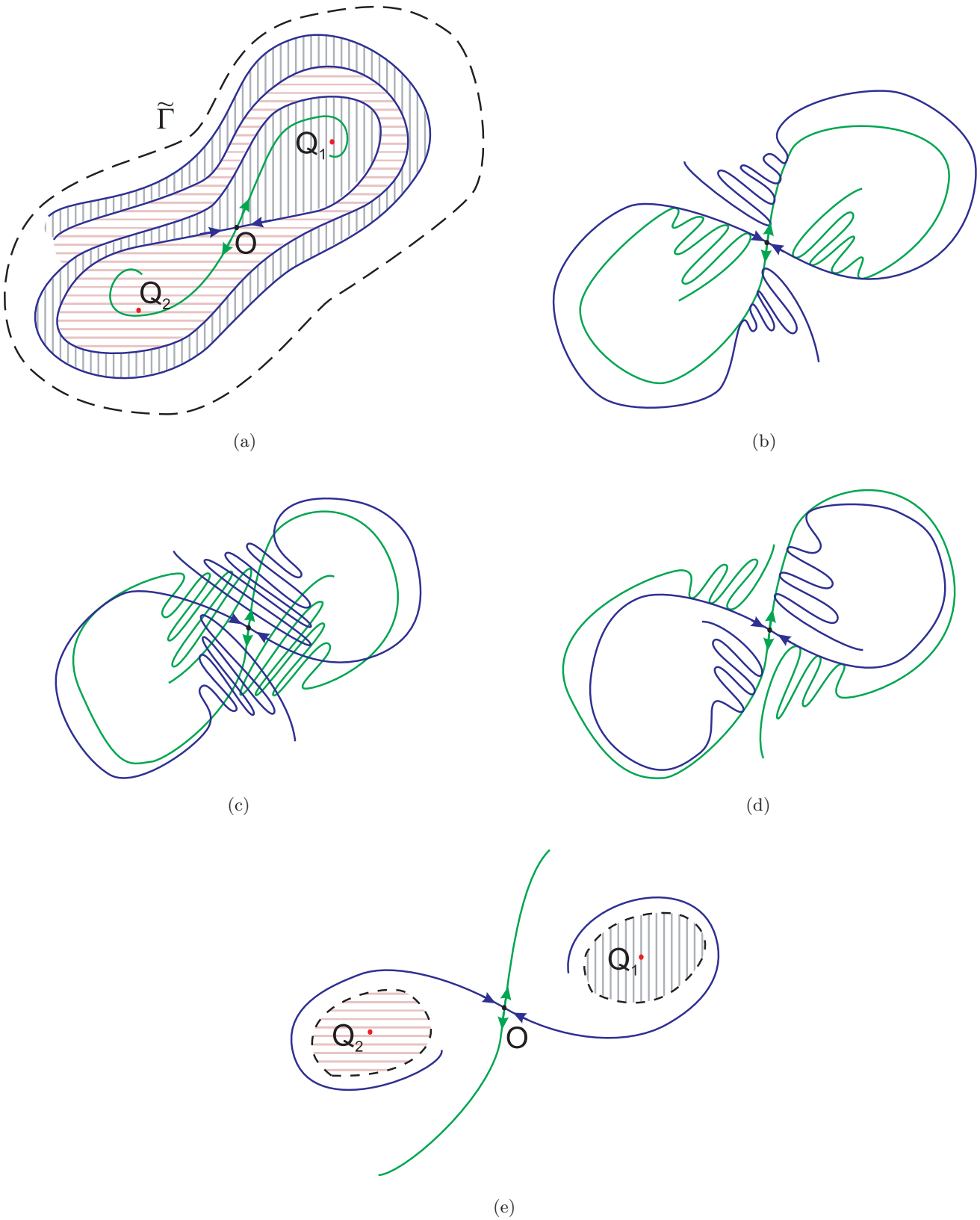

Fig. 3. Qualitative representation of a sequence of global bifurcations leading to the creation of two disjoint repelling closed invariant curve starting from a situation with a unique repelling closed invariant curve. The blue curves represent the stable set of the saddle O, $W^S(O)$, and the green curves represent the unstable set of the saddle O, $W^U(O)$. $W^S(O)$ constitutes the boundary that separates the basins of Q_1 and Q_2.

that separates the basins of Q_1 and Q_2. As the parameters are varied along the path, the repelling closed invariant curve $\tilde{\Gamma}$ shrinks in the proximity of the saddle O, and consequently the stable and unstable sets of the saddle approach each other, until $\tilde{\Gamma}$ disappears or, more precisely, *becomes a chaotic repellor at the homoclinic tangency* [see Fig. 3(b)] at which the unstable set of O, $W^U(O)$, has a contact with the stable one. This homoclinic tangency is followed by a transverse intersections of the two manifolds, $W^U(O)$ and $W^S(O)$, and a dynamic scenario like the one shown in Fig. 3(c) is obtained. Thus the two invariant manifolds form the standard homoclinic tangle, and from the homoclinic theorem for saddles (see e.g. [Guckenheimer & Holmes, 1985; Mira, 1987; Wiggins, 1988; Bai-Lin, 1989; Kuznetsov, 1998]) we know that in this situation a chaotic repellor exists, made up of infinitely many (countable) repelling cycles, of any period, and uncountable aperiodic trajectories. This chaotic repellor, associated with the infinitely many Smale horseshoes existing in the homoclinic tangle, is the limit set of the stable set of the basic fixed point O. Then another homoclinic tangency occurs [see Fig. 3(d)] leading to the disappearance of all the homoclinic orbits of O and of the chaotic repellor: now $W^U(O)$ is completely outside of the stable set. After this tangency the stable and unstable sets are again disjoint, $W^U(O) \cap W^S(O) = \emptyset$, and the preimages of the local stable manifolds reach *two disjoint closed invariant curves which have been created around the two stable fixed points* Q_i, see Fig. 3(e).

In all the pictures of Fig. 3 at least another attracting set exists outside the repelling closed invariant curve $\tilde{\Gamma}$, for example, the stable cycle shown in Fig. 2, whose periodic points are on the attracting closed invariant curve created together with $\tilde{\Gamma}$, or some other attractor. Notice that before the homoclinic tangency the two branches of $W^U(O)$ tend to the two stable fixed points Q_i. During the transverse homoclinic loop some points of $W^U(O)$ tend to Q_i and some points tend to the external attractor. After the second homoclinic tangency, when no homoclinic point of O exists, the whole unstable set of O tends to the external attractor. Before the first homoclinic tangency an infinite number of periodic orbits appear, and they disappear after the second homoclinic tangency.

During the whole sequence described above (the homoclinic tangle) the stable set $W^S(O)$ persists in being the separator between the basins of the two attracting fixed points Q_i, and it has the chaotic repellor as limit set.

2.3. *From one attracting closed invariant curve to a wider one*

In this section we show a mechanism that causes the transition from an attracting closed invariant curve, say Γ_a, with a pair of cycles outside it, a saddle $S_q = \bigcup S_{q,i}$ (where the $S_{q,i}$, $i = 1, \ldots, q$ are the periodic points) and an attracting one, $C_q = \bigcup C_{q,i}$, into another wider attracting closed invariant curve, say Γ_b, with that pair of cycles inside it. This transition takes place via the occurrence of two homoclinic loops of the saddle S_q, first with the merging of the unstable branches $W_1^U(S_q) = \bigcup \alpha_{1,i}$ and the stable ones $W_1^S(S_q) = \bigcup \omega_{1,i}$ and then via the merging of the unstable branches $W_2^U(S_q) = \bigcup \alpha_{2,i}$ and the stable ones $W_2^S(S_q) = \bigcup \omega_{2,i}$. However, more frequently in maps, this transition may occur via two separate homoclinic tangles of S_q, a first one through a homoclinic tangle of $W_1^U(S_q)$ and $W_1^S(S_q)$, which includes a tangency between the two manifolds, followed by transverse crossings, and a tangency again of $W_1^U(S_q)$ and $W_1^S(S_q)$, and a second one through a homoclinic tangle of $W_2^U(S_q)$ and $W_2^S(S_q)$.

We note that, when dealing with a saddle, we use indifferently the term heteroclinic loop (tangle) or homoclinic loop (tangle) because there is substantially no difference. In fact, if we consider the saddle cycle S_q as made up of q fixed points $S_{q,i}$ of the map T^q then we have a cyclical *heteroclinic loop* (*tangle*) *between the fixed points* $S_{q,i}$, and if we consider the cycle S_q of T we may say *homoclinic loop* (*tangle*) *of the cycle* S_q.

Let us consider first the situation described in Fig. 4. In Fig. 4(a) we have an attracting closed invariant curve Γ_a (which may also follow from the situation described in Figs. 2(c) and 2(f) as we shall see in the examples shown in the next section), and a pair of cycles that have been created via a saddle-node bifurcation outside Γ_a. Such external cycles do not form an heteroclinic connection, whereas the stable set of the saddle S_q bounds the basin of attraction of the related attracting fixed points $C_{q,i}$ of the map T^q. The unstable branches $\alpha_{1,i}$ of $S_{q,i}$ tend to the attracting curve Γ_a, while the unstable branches $\alpha_{2,i}$ of $S_{q,i}$ tend to the attracting cycle.

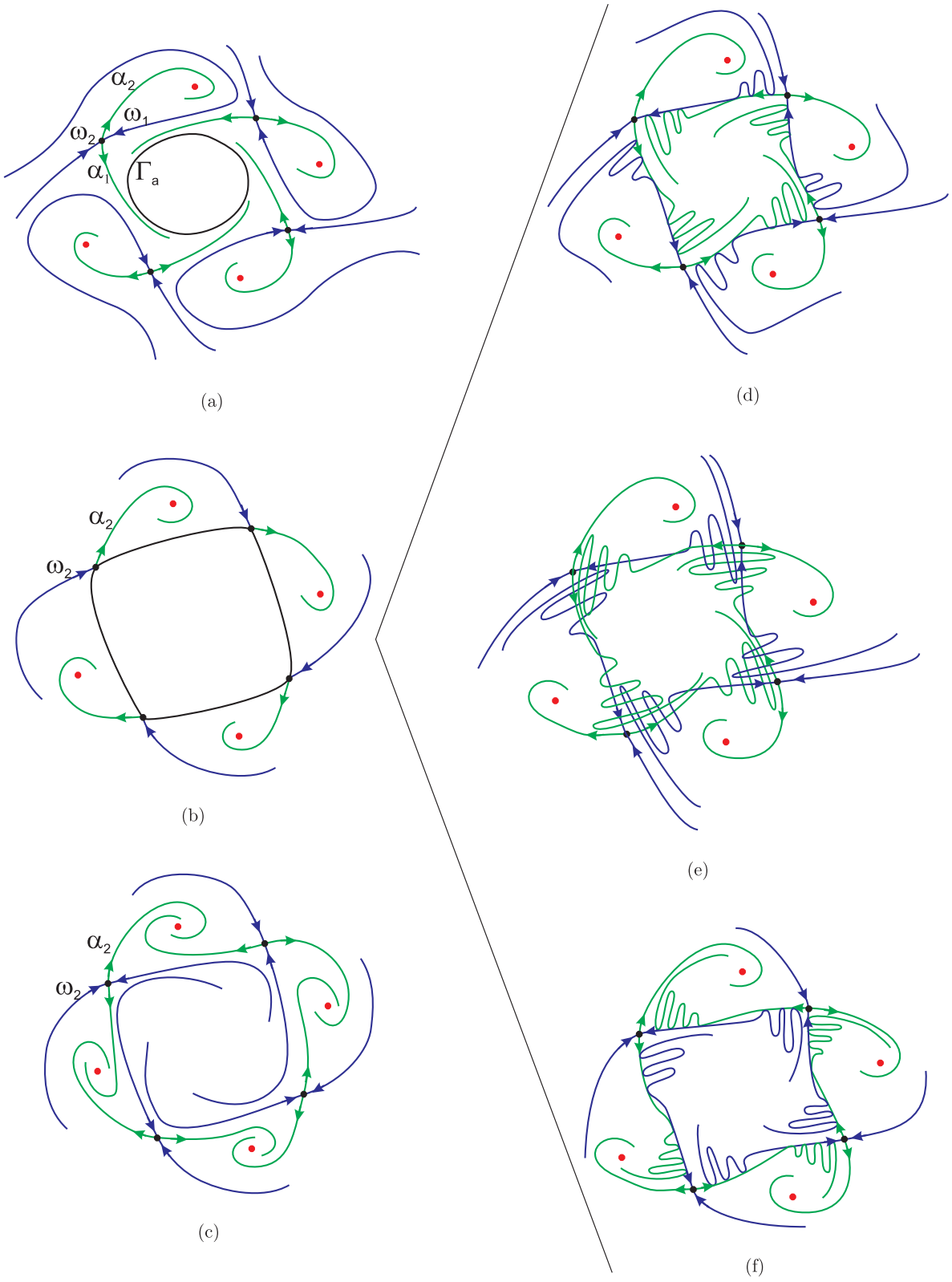

Fig. 4. Qualitative representation of two possible mechanisms that cause the transition from an attracting closed invariant curve Γ_a (a) to a wider attracting closed invariant curve (c). The first mechanism is related to the occurrence of two homoclinic loops of a saddle-cycle (b), the second mechanism, more common when dealing with maps, occurs via two separate homoclinic tangles of the saddle-cycle (sequence (d)–(f)).

At the bifurcation [Fig. 4(b)] we may have that the closed invariant curve Γ_a merges with the unstable branches $W_1^U(S_q) = \bigcup\alpha_{1,i}$ and with the stable ones $W_1^S(S_q) = \bigcup\omega_{1,i}$ as well, in a homoclinic loop of the saddle S_q, causing the disappearance of the attracting closed invariant curve Γ_a, and leaving another closed invariant curve, see Fig. 4(c), which is now the heteroclinic cycle involving the saddle S_q and the related attracting cycle C_q. After the bifurcation of the homoclinic loop a closed curve still exists, but differently from Γ it includes the two cycles on it [Fig. 4(c)].

More frequently in maps, the simple homoclinic loop of the saddle shown in Fig. 4(b) is replaced by a homoclinic tangle of the saddle. That is, from Fig. 4(a) a tangency between the unstable branch $W_1^U(S_q) = \bigcup\alpha_{1,i}$ with the stable one $W_1^S(S_q) = \bigcup\omega_{1,i}$ occurs [Fig. 4(d)], followed by transverse crossings of the two manifolds [Fig. 4(e)], further followed by another tangency of the same manifolds, but on opposite sides, as qualitatively shown in Fig. 4(f), after which the situation of Fig. 4(c) follows.

As already noticed, the saddle cycle S_q corresponds to q fixed points $S_{q,i}$ of the map T^q, and the homoclinic tangle shown in Fig. 4(e), which may be considered associated with q distinct fixed points $S_{q,i}$ of the map T^q, has the same dynamic properties as the homoclinic tangle associated with only one saddle fixed point. This homoclinic bifurcation is also called a *cyclical heteroclinic connection* in the sense of Birkhoff (see [Birkhoff & Smith, 1928]), who first showed that the same properties occur when the stable and unstable manifolds of a saddle fixed point intersect transversely, or when there are two saddle fixed points, say $S_{q,i}$ and $S_{q,j}$, such that $W^S(S_{q,i}) \cap W^U(S_{q,j}) \neq \emptyset$, thus giving cyclical heteroclinic points that form an heteroclinic connection (see also [Gardini, 1994]). In such a case, the transverse intersections of $W^U(S_q)$ and $W^S(S_q)$ for the saddle cycle $S_q = \bigcup S_{q,i}$, called *homoclinic points of nonsimple type* in [Birkhoff & Smith, 1928], gives the same properties as the homoclinic points of a saddle fixed point (called *homoclinic points of simple type* in [Birkhoff & Smith, 1928]). Thus the occurrence of a transverse homoclinic orbit of a saddle cycle is enough to prove the existence of chaotic dynamics, because it is possible to prove that in the neighborhood of any homoclinic orbit there are infinitely many repelling cycles and an invariant "scrambled set" on which the restriction of the map is chaotic in the sense of Li and Yorke (see for example in [Gavrilov & Shilnikov 1972a, 1972b; Wiggins, 1988]).

Before the bifurcation [Fig. 4(a)], the two branches of the stable set of S_q are both outside the closed curve Γ. After this bifurcation, the stable branches $\bigcup\omega_{1,i}$ are inside the closed curve while the stable branches $\bigcup\omega_{2,i}$ are outside, and approach the unstable branches $\bigcup\alpha_{2,i}$ [Fig. 4(c)]. Starting from this situation [reported in Fig. 5(a)], a second homoclinic loop [Fig. 5(b)] or tangle [Figs. 5(d)–5(f)] may be formed. The heteroclinic connection turns into a homoclinic loop in which the unstable branches $W_2^U(S_q) = \bigcup\alpha_{2,i}$ merge with the stable ones $W_2^S(S_q) = \bigcup\omega_{2,i}$ [see Fig. 5(b)]. After the bifurcation a new closed attracting curve exists, say Γ_b, and the two cycles are both inside Γ_b [Fig. 5(c)]. The stable set of the saddle S_q separates the basins of attraction of the q attracting fixed points of the map T^q. The unstable branches $\bigcup\alpha_{1,i}$ tend to the attracting cycle while the unstable branches $\bigcup\alpha_{2,i}$ tend to Γ_b.

As mentioned before, in the case of maps the dynamic behaviors more frequently observed indicate that the homoclinic loop of Fig. 5(b) is often replaced by a homoclinic tangle of the outer manifolds $W_2^U(S_q)$ and $W_2^S(S_q)$. That is, a tangency occurs between the two manifolds [Fig. 5(d)] followed by transverse intersections [Fig. 5(e)] and a tangency again on the opposite side [Fig. 5(f)] after which all the homoclinic points of the saddle S_q, created before the first homoclinic tangency, are destroyed.

It is worth noticing that all the unstable periodic points associated with the first homoclinic tangle, due to $W_1^U(S_q) \cap W_1^S(S_q) \neq \emptyset$ [Fig. 4(e)], are in the region interior to the set of periodic points of the saddle S_q, whereas in the strange repellor associated with the second homoclinic tangle, in which $W_2^U(S_q) \cap W_2^S(S_q) \neq \emptyset$ [Fig. 5(e)], all the unstable cycles are "outside" the saddle cycle S_q.

Notice also that before the homoclinic loop (tangle) of Fig. 4 we have two distinct attracting sets: Γ_a and the stable q-cycle outside it; after the homoclinic loop (tangle) of Fig. 5, we have again two distinct attractors: Γ_b, which is wider than Γ_a, and the q-cycle inside it.

It is plain that this process may be repeated many times. In fact, by a saddle-node bifurcation a new pair of cycles may appear outside Γ_b, so that we are again in the situation of Fig. 4(a), and the sequence of bifurcations described in Figs. 4 and 5 may repeat. Indeed, this repeated occurrence

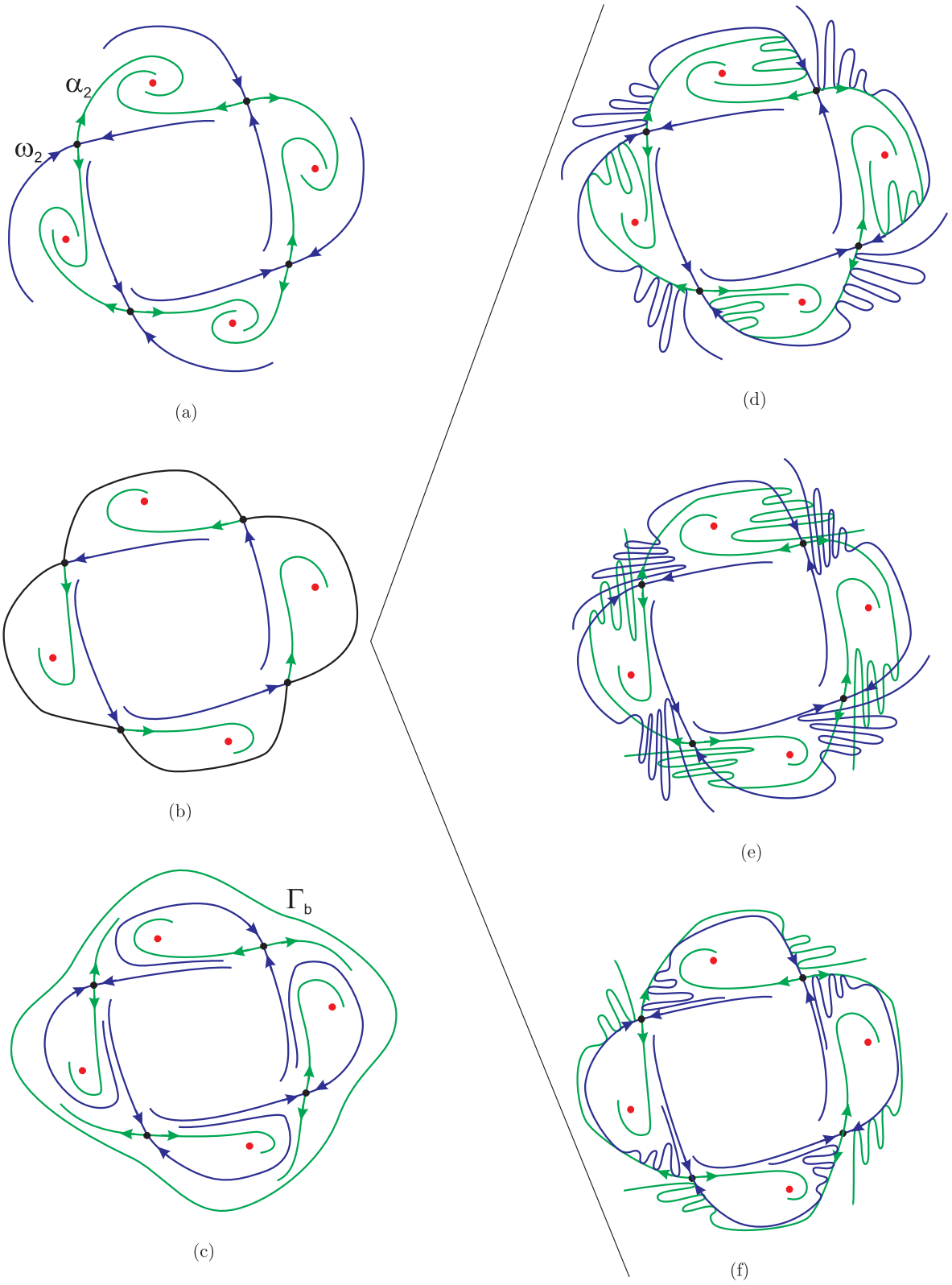

Fig. 5. Starting from the situation in Fig. 4(c), reported in (a), two possible mechanisms that cause the transition to a wider attracting closed invariant curve, represented in (c), are shown. In (b) the transition occurs via a homoclinic loop, in (d)–(f) via homoclinic tangles.

will be seen in the numerical examples of the next sections.

We remark that also the homoclinic loops represented in Figs. 2(b) and 2(e) may be replaced by homoclinic tangles, like the ones shown in Figs. 4(d)–4(f) and 5(d)–5(f).

We finally remark that the sequence of bifurcations here described, that cause the transition of a pair of cycles from outside to inside a closed invariant curve, may occur through different mechanisms when the map is noninvertible. In fact, in noninvertible maps the invariant curve may intersect the critical set LC_{-1}[1], and when this occurs the periodic points of a cycle may be part inside and part outside the closed invariant curve (see [Mira *et al.*, 1996; Frouzakis *et al.*, 1997]).

2.4. *Coexistence of two closed invariant curves and two cycles in between*

In the situation described in Fig. 5(c) we may also have a repelling closed curve $\tilde{\Gamma}$ inside (as in fact it occurs if the bifurcation follows from the sequence in Fig. 2, as seen in the examples). Thus the resulting picture in Fig. 5(c) may be that of two closed invariant curves, say the attracting Γ outside and the repelling $\tilde{\Gamma}$ inside, and a pair of cycles between them, a saddle S_q and the related attracting cycle C_q.

A different mechanism, which may lead to the same qualitative results is obtained starting from the situation described in Figs. 2(c) and 2(f), where we have an attracting heteroclinic connection surrounding the repelling closed curve $\tilde{\Gamma}$ (created via the homoclinic loop/tangle of the manifolds $\bigcup\alpha_{1,i}$ and $\bigcup\omega_{1,i}$) and we are also in the situation described in Fig. 5(a). Thus another attracting set may be created via a homoclinic loop/tangle in which the unstable branches $\bigcup\alpha_{2,i}$ merge with the stable ones $\bigcup\omega_{2,i}$ (see Fig. 5(b), or Figs. 5(d)–5(f)). After the bifurcation [Fig. 5(c)] a new attracting closed invariant curve exists, say Γ, and the two cycles of period q are both between the two closed curves Γ and $\tilde{\Gamma}$. The stable set of the saddle cycle S_q separates the basins of attraction of the q attracting fixed points of the map T^q. The unstable branches $\bigcup\alpha_{1,i}$ tend to the attracting cycle, while the unstable branches $\bigcup\alpha_{2,i}$ tend to Γ.

2.5. *Coexistence of several repelling closed invariant curves*

In this section we show a mechanism which may cause the appearance of cyclical closed invariant curves. This mechanism is known in the literature, see e.g. [Mira, 1987; Kuznetsov, 1998], however we give here its description in order to comment what may happen when a pair of cycles, a saddle S_q and the related stable cycle C_q, are located between the closed invariant curves Γ and $\tilde{\Gamma}$ already seen in the situations described before. For example, let us consider the situation shown in Fig. 6(a). When the stable cycle is an attracting focus, we may observe an homoclinic loop in the invariant manifold of the saddle, in which the branch $\alpha_{1,i}$ merges with $\omega_{2,i}$, for each i, i.e. in each periodic point of the saddle S_q [Fig. 6(b)]. After the bifurcation q repelling closed invariant curves appear around the cycle focus, which constitute the boundary of the immediate basin of attraction of the q attracting fixed points of the map T^q [Fig. 6(c)]. Now both the unstable branches of the saddle S_q tend to the attractor outside, i.e. the closed curve Γ.

To close this section we remark that also in this case the homoclinic loop qualitatively represented in Fig. 6(b) may be replaced by an homoclinic tangle between the two manifolds $W_1^U(S_q) = \bigcup\alpha_{1,i}$ and the stable one $W_2^S(S_q) = \bigcup\omega_{2,i}$: a tangency, followed by transverse crossings that gives homoclinic points of the saddle S_q, followed by a second tangency between the same manifolds at which the transverse homoclinic points of S_q disappear.

[1]A specific feature of noninvertible maps is the existence of the *critical set LC*, defined as the locus of points having at least two coincident rank-1 preimages, located on the set of merging preimages denoted by LC_{-1}. For a continuously differentiable map LC_{-1} belongs to the set of points where the Jacobian determinant vanishes. Segments of LC are boundaries that separate different regions Z_k, whose points have k distinct rank-1 preimages, see [Gumowski & Mira, 1980; Mira *et al.*, 1996].

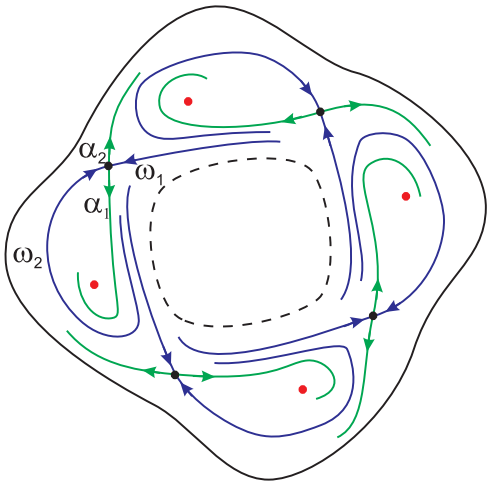

(a)

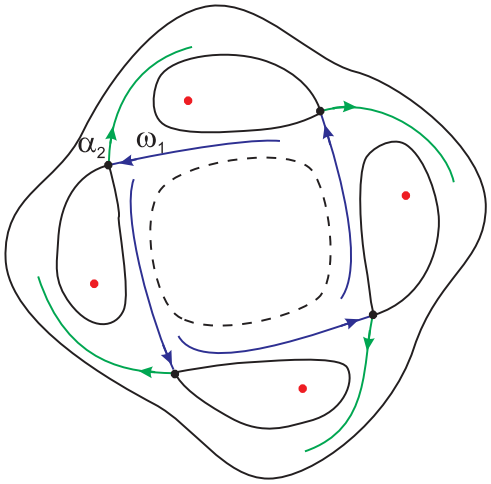

(b)

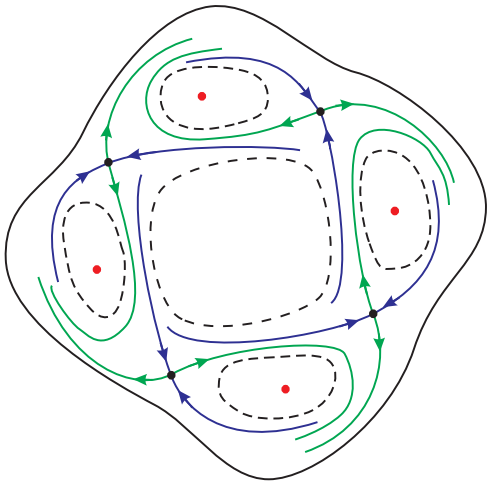

(c)

Fig. 6. Qualitative representation of a mechanism which may cause the appearance of cyclical closed invariant curves.

3. A Family of Symmetric Maps

The first family of two-dimensional maps, that we propose for a numerical exploration of the bifurcations described in Sec. 2, is:

$$T: \begin{cases} x' = ax + y \\ y' = bx + cy + d \cdot \arctan y \end{cases} \tag{1}$$

where we assume $0 < a < 1$ and $d > 0$. Maps which exhibit the same qualitative properties of (1) can be easily found in applications, see for example [Herrmann, 1985; Lorenz, 1992; Bischi *et al.*, 2001; Dieci *et al.*, 2001; Bischi *et al.*, 2003]. It is worth noticing that also changing the function $\arctan(\cdot)$ with any other function having an S-shaped graph, we obtain the same kind of bifurcations as those described in this section.

The map (1) has a fixed point in the origin O, and two more fixed points, say Q_1 and Q_2, exist if the parameters satisfy the condition:

$$m := \frac{(1-c)(1-a) - b}{d(1-a)} < 1 \tag{2}$$

and have coordinates (x_i, y_i), $i = 1, 2$, where $x_i = y_i/(1-a)$ and y_i are the nonzero solutions of the equation $my - \arctan(y) = 0$. The stability region of the fixed point O is obtained from the analysis of the eigenvalues of the Jacobian matrix of T, given by

$$DT(x, y) = \begin{bmatrix} a & 1 \\ b & c + \dfrac{d}{1+y^2} \end{bmatrix},$$

evaluated in O:

$$DT(O) = \begin{bmatrix} a & 1 \\ b & c+d \end{bmatrix}. \tag{3a}$$

Let $\mathcal{P}(z) = z^2 - \mathrm{Tr}z + \mathrm{Det}$ be the characteristic polynomial, where Tr and Det denote the trace and the determinant of $DT(O)$ respectively. Then the stability region of O is determined by the following conditions (see e.g. [Gumowski & Mira, 1980, p. 159] or [Medio & Lines, 2001, p. 52], or any standard book on discrete dynamical systems): $\mathcal{P}(1) = 1 - \mathrm{Tr} + \mathrm{Det} > 0$, $\mathcal{P}(-1) = 1 + \mathrm{Tr} + \mathrm{Det} > 0$, $\mathrm{Det} < 1$. This region is represented by the gray-shaded triangle in Fig. 7(a). Simple computations show the pitchfork bifurcation curve **P**, defined by the equation $\mathcal{P}(1) = 0$, has equation $b = (1-a)(1-c-d)$, i.e. a straight line in the (c, b) parameter plane, assuming a and d at fixed

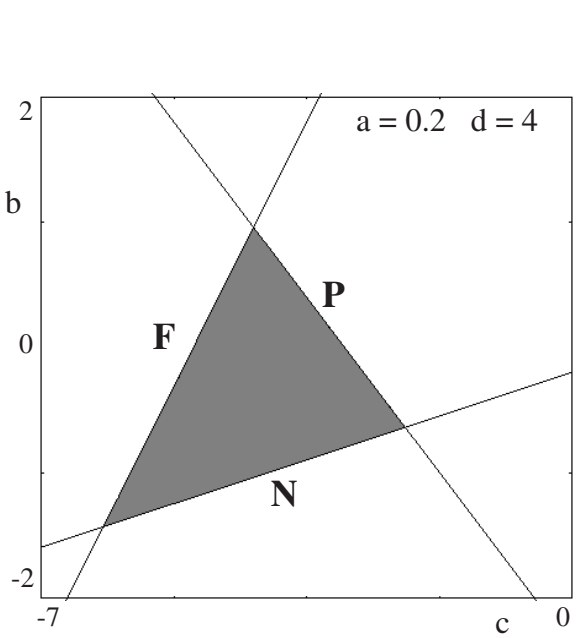

(a)

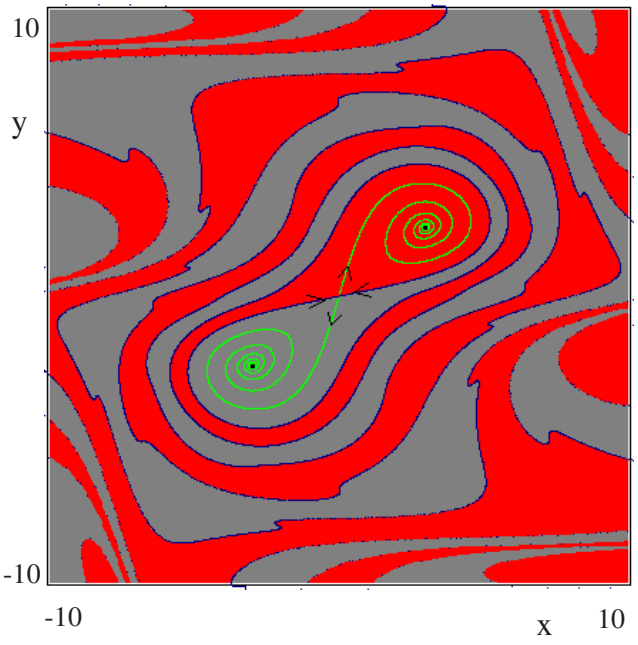

(b)

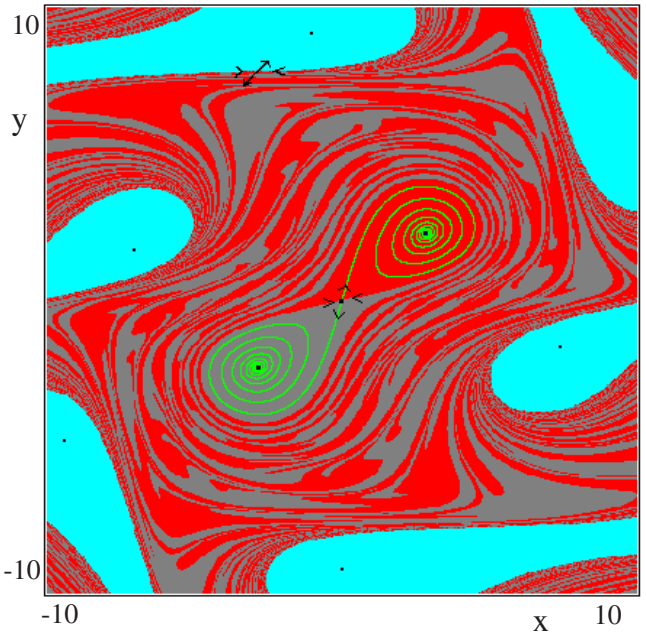

(c)

Fig. 7. For the map (1), with $a = 0.2$ and $d = 4$, in (a) the stability region of the basic fixed point $O = (0, 0)$, is represented in the space of the parameters c and b by a gray-shaded triangle, bounded by the pitchfork bifurcation curve **P**, the flip bifurcation curve **F** and the Neimark bifurcation curve **N**. (b) For $a = 0.2$, $d = 4$, $c = -0.1$ and $b = -0.7$, the basins $B(Q_1)$ and $B(Q_2)$ of the two stable focuses Q_1 and Q_2 are numerically obtained, represented by gray and red regions, respectively. The blue curve represent the stable set $W^S(O)$ of the saddle O, the green curve represents the unstable set $W^U(O)$. (c) For the same values of the parameters a, d, c as in figure (b), and with $b = -0.75$, a stable cycle of period 6 exists, whose numerically computed basin of attraction is represented by pale blue regions.

values, see the curve **P** in Fig. 7(a). The flip bifurcation curve, defined by $\mathcal{P}(-1) = 0$, has equation $b = (1 + a)(1 + c + d)$, again a straight line in the (c, b) parameter plane. The Neimark bifurcation curve, defined by Det = 1, corresponds to $b = a(c + d) - 1$, another straight line in the (c, b) parameter plane.

The map (1) is symmetric with respect to the origin, because $T(-x, -y) = -T(x, y)$. This implies that any invariant set of T is either symmetric with respect to O, or it admits a symmetric invariant set. In particular, this holds for the fixed points and cycles of T. Thus the two fixed points Q_i, when they exist, are in the symmetric positions with respect to O, and any cycle of T of odd period necessarily coexists with a symmetric one having the same characteristics. For the same reason also all the basins of attraction are either symmetric with respect to O or another basin also exists in symmetric position.

We also notice that the map T can be invertible or noninvertible, according to the set of parameters considered. In fact, looking for the preimages of a point (x', y') we get $x = (x' - y)/a$ where y is the solution of the equation:

$$\frac{ay' - bx'}{ad} + \frac{b - ac}{ad} y = \arctan(y) \tag{4}$$

Equation (4) admits a unique solution for any (x', y') (i.e. any point (x', y') has a unique preimage) when $(b - ac)/ad \leq 0$ or $(b - ac)/ad \geq 1$, while in the case $0 < (b - ac)/ad < 1$, i.e. $ac < b < ac + ad$, (4) may admit one or three solutions depending on (x', y') (which means that both points (x', y') with one preimage and points (x', y') with three preimages exist). Moreover, from the Jacobian determinant $\det DT(x, y) = (ac - b) + ad/(1 + y^2)$ we see that it vanishes on two straight lines of the plane, $y = \pm\sqrt{ad/(b - ac) - 1}$, when the following condition holds:

$$\frac{ad}{b - ac} - 1 > 0. \tag{5}$$

Thus, when the parameters are taken in the strip $ac < b < ac + ad$ of the (c, b) parameter plane, then map T is noninvertible of type $Z_1 - Z_3$. Following the terminology of [Mira *et al.*, 1996] this means that as (x', y') vary in the phase plane, Eq. (4) can have one or three real solutions. However, the parameter values that we shall use in the examples of the following sections always belong to the region in which T is invertible.

In the following, we consider some sequences of numerical simulations obtained with fixed values of $a = 0.2$, $c = -0.1$ and $d = 4$, and we gradually decrease the parameter b.

3.1. *Appearance of cycles and two closed invariant curves*

Let us start with a value of the parameter b out of the stability region, not far from the pitchfork bifurcation curve **P**, so that the fixed point O is a saddle, and the two fixed points Q_1 and Q_2 are stable. The two branches of the unstable set of the saddle O tend to these fixed points, while the stable set of O separates their basins of attraction. This is the situation shown in Fig. 7(b), obtained with $b = -0.7$, where the basin $B(Q_1)$ is represented by the gray region and the basin $B(Q_2)$ is the red region. The evident convolutions of the stable set $W^S(O)$ (the blue line) suggest that a pair of cycles is going to appear by saddle-node bifurcation. Indeed, in Fig. 7(c), obtained for $b = -0.75$, we can see that besides the two basins $B(Q_i)$, separated by $W^S(O)$ another attractor exists: a 6-cycle C_6, whose basin is made up of 6 disjoint areas (the pale-blue regions) bounded by the stable set $W^S(S_6)$ of the 6-cycle saddle S_6 born with C_6. In Fig. 7(c) we can also see that the stable set $W^S(O)$ has many oscillations, and a further decrease of b causes the creation of another pair of cycles. In fact, in Fig. 8(a), besides the basins $B(Q_1)$, $B(Q_2)$ and $B(C_6)$, we see also the basin $B(C_{10})$ (yellow) of an attracting cycle of period 10, which is born together with a saddle S_{10} whose stable set $W^S(S_{10})$ gives the boundary of the basin $B(C_{10})$. $B(C_{10})$ becomes wider as b decreases, as shown in Fig. 8(b), where $B(Q_1)$ and $B(Q_2)$ have thin tongues, bounded by $W^S(O)$, inside the $B(C_{10})$.

Up to now we have four coexisting attractors but no closed invariant curves (all the stable sets are basins separators, and the unstable branches $W_1^U(S_q)$ and $W_2^U(S_q)$, $q = 6, 10$, have different limit sets). However in the enlargement of a portion of Fig. 8(b), shown in Fig. 8(c), we can see many convolutions of $W^S(O)$ in the region close to the cycle S_{10}. This is a sign that something is going to appear as b is further decreased, and in fact in Fig. 9(a) (and its enlargement, Fig. 9(c)) we can see that a pair of closed invariant curves exist, say Γ (attracting) and $\tilde{\Gamma}$ (repelling). Now $W^S(O)$ cannot exit the region bounded by $\tilde{\Gamma}$ (i.e. the preimages of the local stable manifolds of $W^S(O)$ have $\tilde{\Gamma}$ as limit set). The

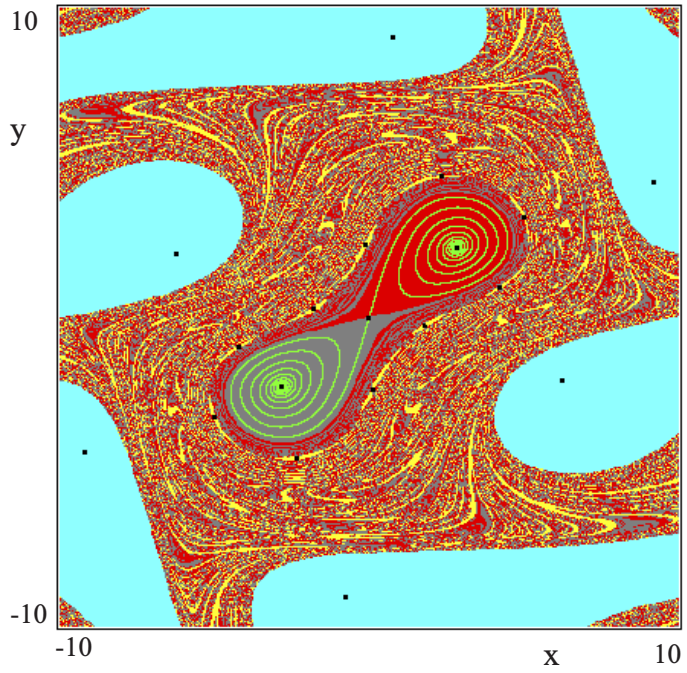

(a)

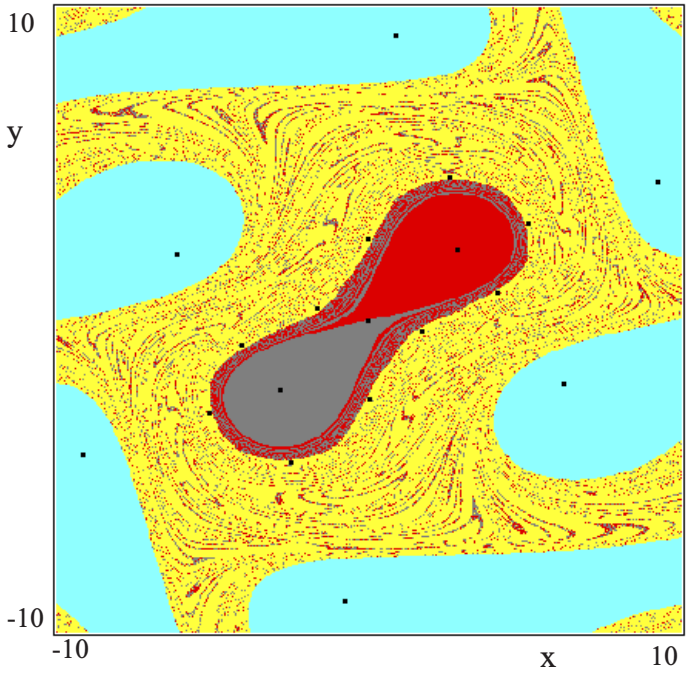

(b)

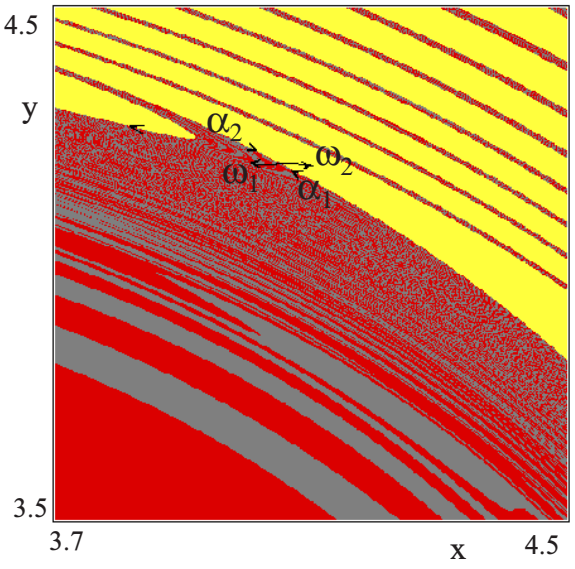

(c)

Fig. 8. (a) With $b = -0.764$, the basins $B(Q_1)$, $B(Q_2)$ and $B(C_6)$ are represented by gray, red and pale blue, respectively, like in Fig. 7(c), together with the yellow basin $B(C_{10})$ of an attracting cycle of period 10. (b) For $b = -0.7649$ the basins $B(Q_1)$ and $B(Q_2)$ have thin tongues inside $B(C_{10})$. (c) Enlargement of a portion of figure (b).

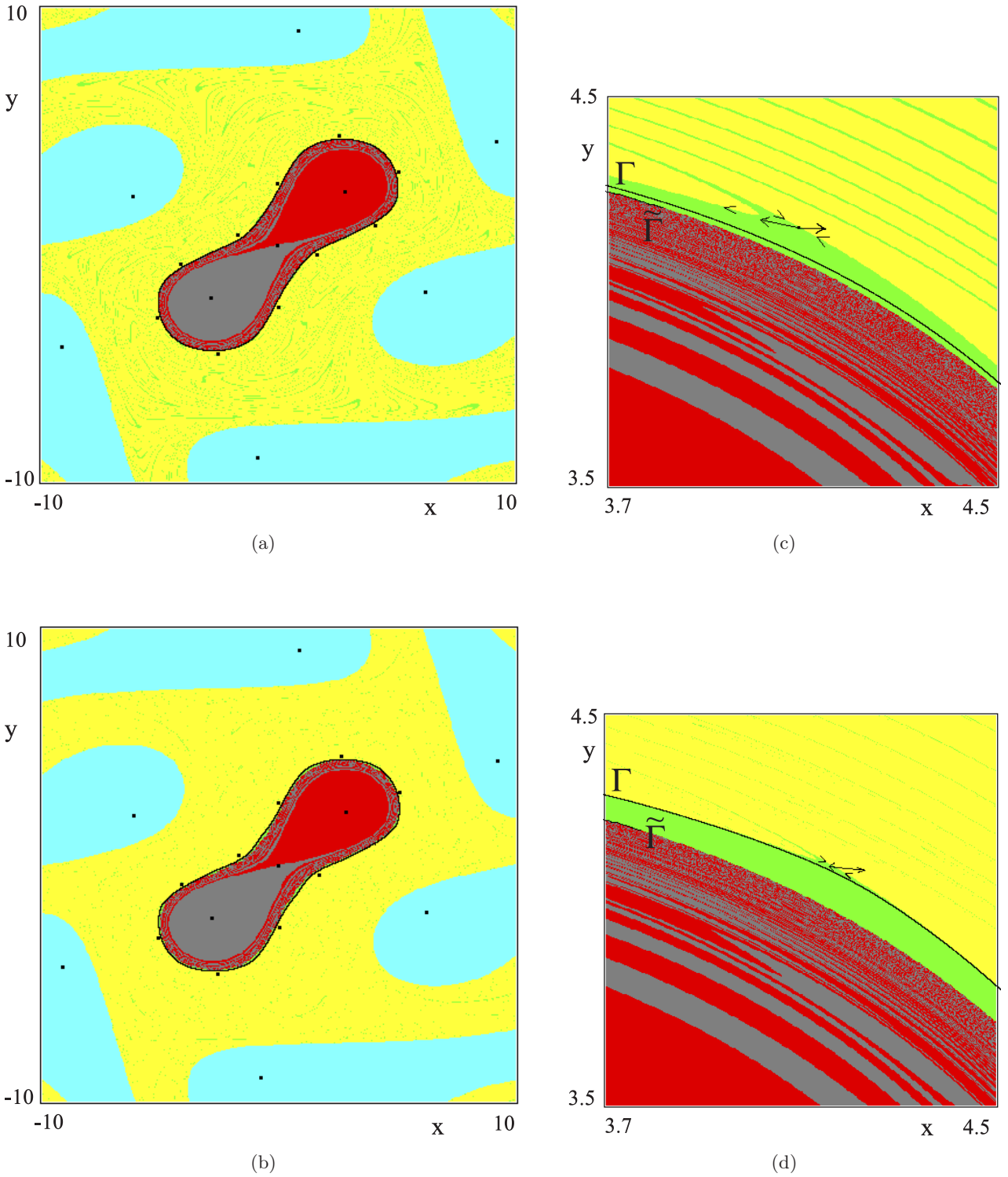

Fig. 9. (a) For $b = -0.76494$ an attracting closed invariant curve Γ exists, whose basin, represented by green color, is bounded by a repelling closed invariant curve $\tilde{\Gamma}$ and the stable set $W^S(S_{10})$. (b) Enlargement of a portion of figure (a). (c) $b = -0.76494$, (d) enlargement of a portion of figure (c).

basin of the new attractor Γ (the green region in Fig. 9) is bounded by $\tilde{\Gamma}$ on one side and by the stable set of the saddle S_{10}, $W^S(S_{10})$, on the other side. That is, $W^S(S_{10})$ separates the yellow basin of the cycle C_{10} from the green basin of Γ, and $\tilde{\Gamma}$ separates the basins of Q_1 and Q_2 (gray and red respectively) from the green basin of Γ. The bifurcation that leads to the appearance of the two closed invariant curves Γ and $\tilde{\Gamma}$ may be a saddle-node bifurcation for closed curves, however it is more likely that (as it occurs in the other examples) the mechanism is the one shown in Fig. 2, with homoclinic loop/tangle, associated with a cycle of very high period, and all occurring in a very narrow range of the parameter b.

3.2. *Transition to cycles between two closed invariant curves*

As b is further decreased, the closed attracting curve Γ approaches the saddle cycle S_{10}, as shown in Figs. 9(b) and 9(d), and the two bifurcations that we have qualitatively described in Figs. 4 and 5 are now going to occur. First, the merging of Γ with the homoclinic connection of the saddle cycle S_{10} (probably via an homoclinic tangle) causes the disappearance of the attracting set Γ, leaving a saddle-focus connection between the cycles C_{10} and S_{10}. This is the situation in Fig. 10(a), where the green basin no longer exists. In the enlargement shown in Fig. 10(b) we can see that the yellow basin of the cycle C_{10} is shared amongst the 10 fixed points $C_{10,i}$ of the map T^{10}, represented by different colors in order to stress that the branches of the manifolds $W_2^U(S_{10})$ and $W_2^S(S_{10})$ are very close, so that we are moving towards the occurrence of the bifurcation qualitatively described in Fig. 5.

In fact, if b is slightly decreased another attracting closed invariant curve is created outside the cycle C_{10}, whose basin (yellow) is a narrow strip [see Fig. 11(a)] and the basin of the new attractor Γ (green region) is bounded on one side by the stable set $W^S(S_6)$ (that separates green and blue) and on the other side is bounded by the stable set $W^S(S_{10})$ (that separates green and yellow). In the enlargement shown in Fig. 11(b) we can see that, according to the qualitative description of Fig. 5, both the cycles C_{10} and S_{10}, as well as the whole stable set $W^S(S_{10})$, belong to the strip between the closed invariant curves Γ and $\tilde{\Gamma}$, $W_1^U(S_{10})$ tends to the cycle C_{10} while $W_2^U(S_{10})$ tends to Γ.

3.3. *Transition from one repelling closed curve to two disjoint repelling curves*

Continuing to decrease the parameter b, starting from the situation in Fig. 11, the cycle C_{10} disappears (via a saddle-node bifurcation, merging with the saddle S_{10}), and the basin $B(\Gamma)$ is separated from the two basins $B(Q_i)$ by the closed repelling curve $\tilde{\Gamma}$, which is the α-limit set of the saddle O. However, the closed repelling curve $\tilde{\Gamma}$ shrinks near the origin (see Fig. 12) and the homoclinic bifurcation of O, qualitatively described in Fig. 3, is going to occur. In order to see what happens in the range of b where the homoclinic tangle develops, in Fig. 13 we show some enlargements of the numerical explorations obtained by decreasing the parameter b starting from the value used in Fig. 12.

In the enlargement of the region around the saddle fixed point O, shown in Fig. 13(a), we can see the first homoclinic tangency between $W^U(O)$ and $W^S(O)$. The whole branch of unstable set on the right belongs to the red basin and tends to the fixed point Q_2, the symmetric one belongs to the gray region and tends to the fixed point Q_1. Both are represented as a whole in Fig. 14(a), at the same parameter value. The stable set $W^S(O)$ already has a complex structure: the closed invariant repelling curve $\tilde{\Gamma}$ is replaced by a strange repellor, which separates the two basins $B(Q_i)$ from $B(\Gamma)$ (yellow points).

Figure 13(b) shows the transverse crossings between $W^S(O)$ and $W^U(O)$. Such intersections are homoclinic points of O. The stable set $W^S(O)$ still is the separator between the two basins $B(Q_i)$ and now its limit set is a chaotic repellor, associated with the infinitely many periodic points existing close to the homoclinic trajectories (i.e. the scrambled repelling sets associated with the Smale horseshoes of the homoclinic tangle). In Fig. 13(b) we can notice that the unstable set $W^U(O)$ now includes points in the basin of the closed attracting curve Γ (the green points inside the yellow region) as well as points belonging to the basins of the two fixed points (green dots in the red or gray regions). The whole picture of $W^U(O)$, for the same set of parameters as in Fig. 13(b) is shown in Fig. 14(b).

As b is further decreased, more and more points of $W^U(O)$ enter the yellow region, and when the tangency on the other side occurs, as shown in Fig. 13(c), the ω-limit set of $W^U(O)$ no longer includes the steady states, but only the closed

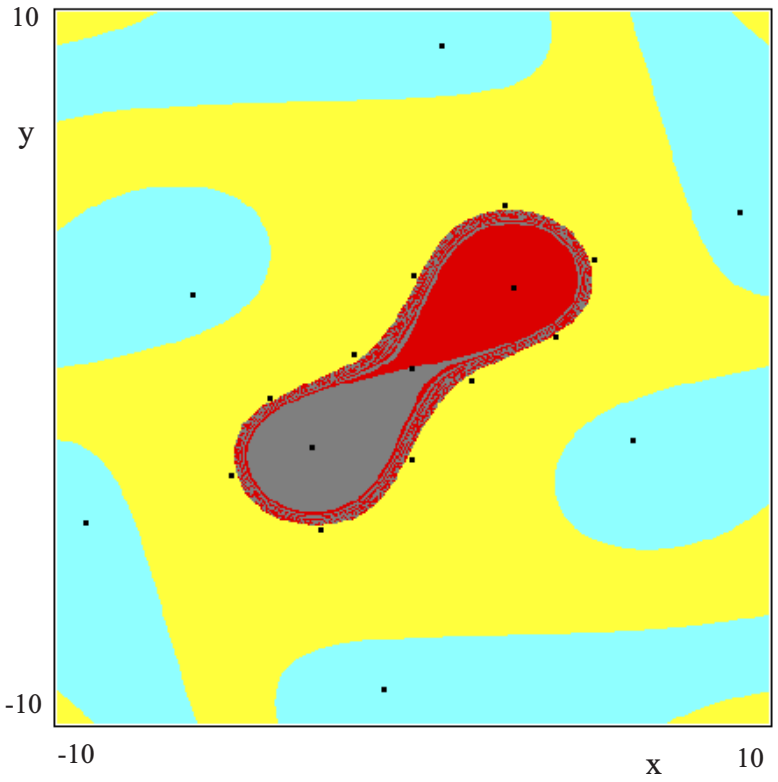

(a)

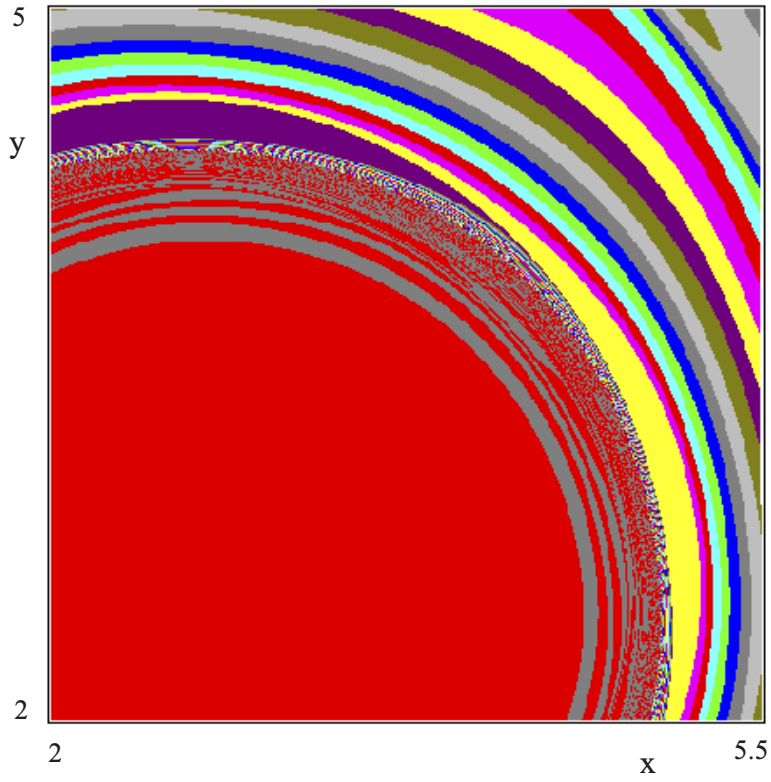

(b)

Fig. 10. (a) Basins and attractors for $b = -0.765$. (b) Enlargement of a portion of figure (a) where different colors are used to represent the basins of the 10 fixed points for the map T^{10}, separated by $W^S(S_{10})$.

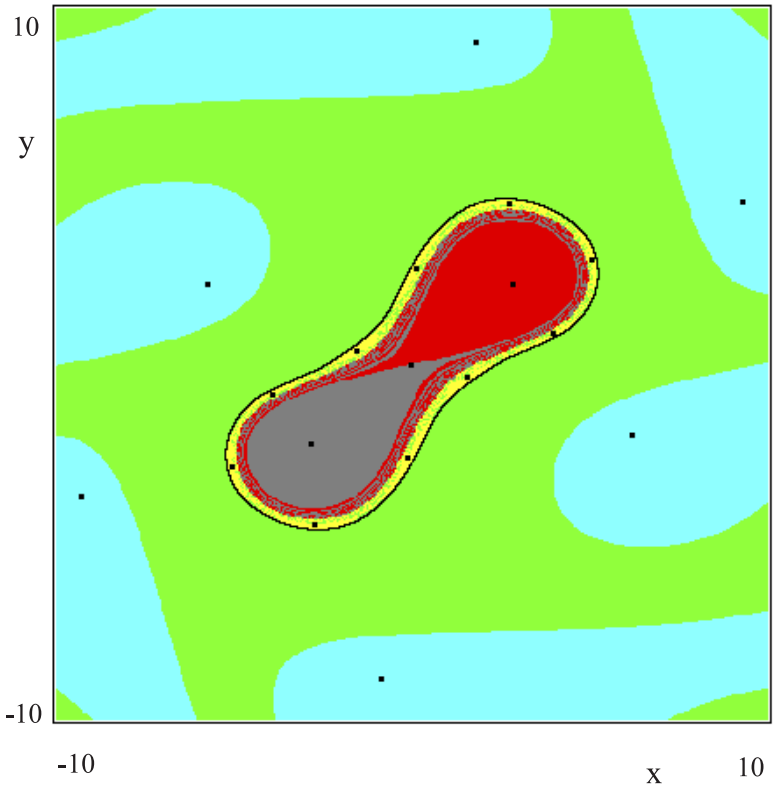

(a)

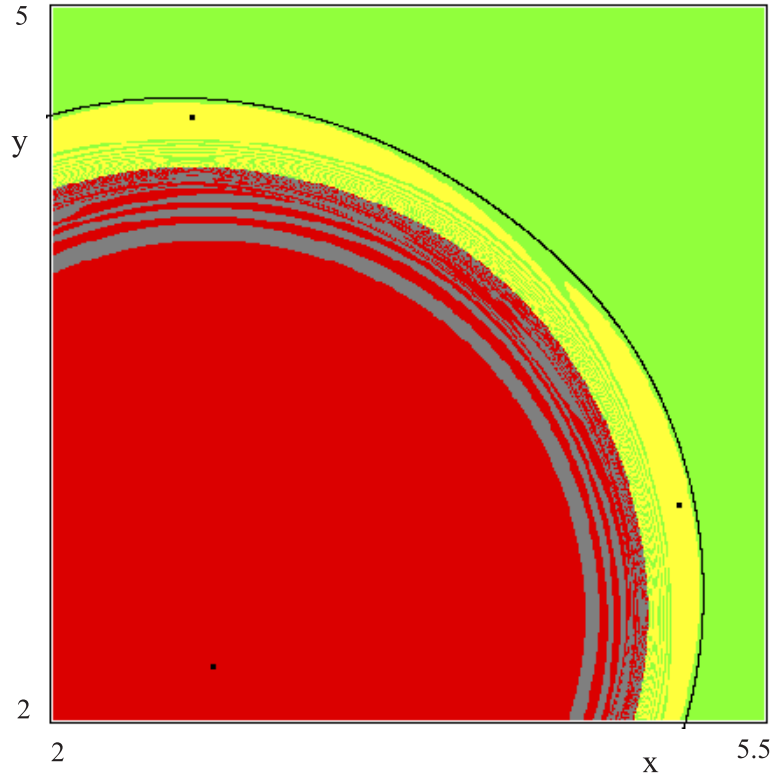

(b)

Fig. 11. (a) For $b = -0.7655$ an attracting closed invariant curve, whose basin is green, exists around the cycle C_{10}, whose basin is yellow. (b) Enlargement of a portion of figure (a).

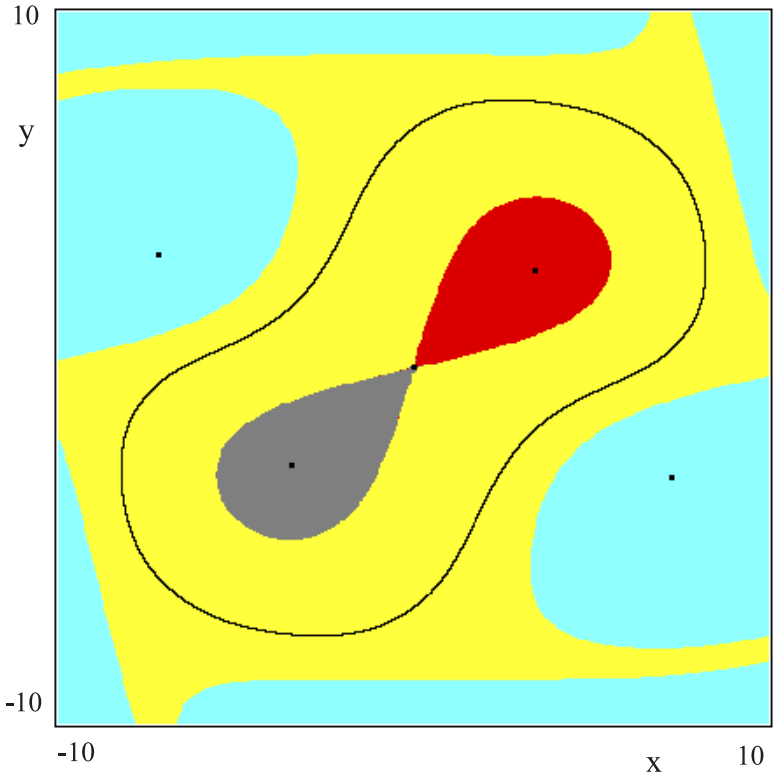

Fig. 12. $b = -0.791468$.

attracting curve Γ, as shown in Fig. 14(c). This closes the homoclinic tangle. After this tangency $W^U(O) \cap W^S(O) = \emptyset$, that is no homoclinic points of O survive, and also the chaotic repellors disappear, leaving two disjoint repelling closed invariant curves $\tilde{\Gamma}_i$ as basin boundaries of the fixed points Q_i. After the homoclinic tangle of O the preimages of the stable set have as limit set the two disjoint closed invariant curves $\tilde{\Gamma}_i$ while the unstable set tends to Γ. An example of the surviving attracting sets and their basins is shown in Fig. 15(a), obtained after a further decrease of the parameter b.

3.4. *Transition from attracting closed invariant curves to wider ones*

In Fig. 15(a) we have a saddle cycle S_6 such that its stable set $W^S(S_6)$, represented in blue in Fig. 15(b), separates the basin of the stable cycle C_6 (pale blue region) from the basin of the attracting closed curve Γ (yellow region). Moreover, we can see that the six disjoint portions of $B(C_6)$ are approaching each other as b is decreased, which means that the branches $W_1^U(S_6)$ and $W_1^S(S_6)$ are approaching (the unstable set $W_1^U(S_6)$ of the saddle cycle is represented in green in Fig. 15(b)) and also the attracting curve Γ is approaching the stable set $W_1^S(S_6)$ of the saddle. As b is decreased, the occurrence of the homoclinic tangle qualitatively described in Fig. 4 is numerically observed [see Figs. 15(c) and 15(d)]. Indeed, the enlargement shown in Figs. 15(e) and 15(f), puts in evidence the first homoclinic tangle, as $W_1^U(S_6) \cap W_1^S(S_6) \neq \emptyset$. At the end of the tangle, i.e. after the second tangency, the attracting curve Γ no longer exists. The attractors are the cycle C_6 and the two fixed points Q_i. Figure 15(g) shows the situation after this first homoclinic tangle, and the colors refer to the basins of the 6 fixed points for the map T^6, and Fig. 15(h) shows the stable and unstable sets of the saddle S_6, which are without intersections, i.e. no homoclinic points of the saddle survive. A closed invariant curve still exists, formed by the saddle-focus connection, or heteroclinic connection, of the cycles S_6 and C_6. The two branches of the unstable set of the periodic points of S_6 reach two different periodic points of the cycle C_6 (green curve in Fig. 15(h)), while the stable set $W_1^S(S_6)$ (blue curve in Fig. 15(h)) separates the 6 basins and approaches the repelling closed invariant curves, that is, the boundaries of the two basins $B(Q_i)$.

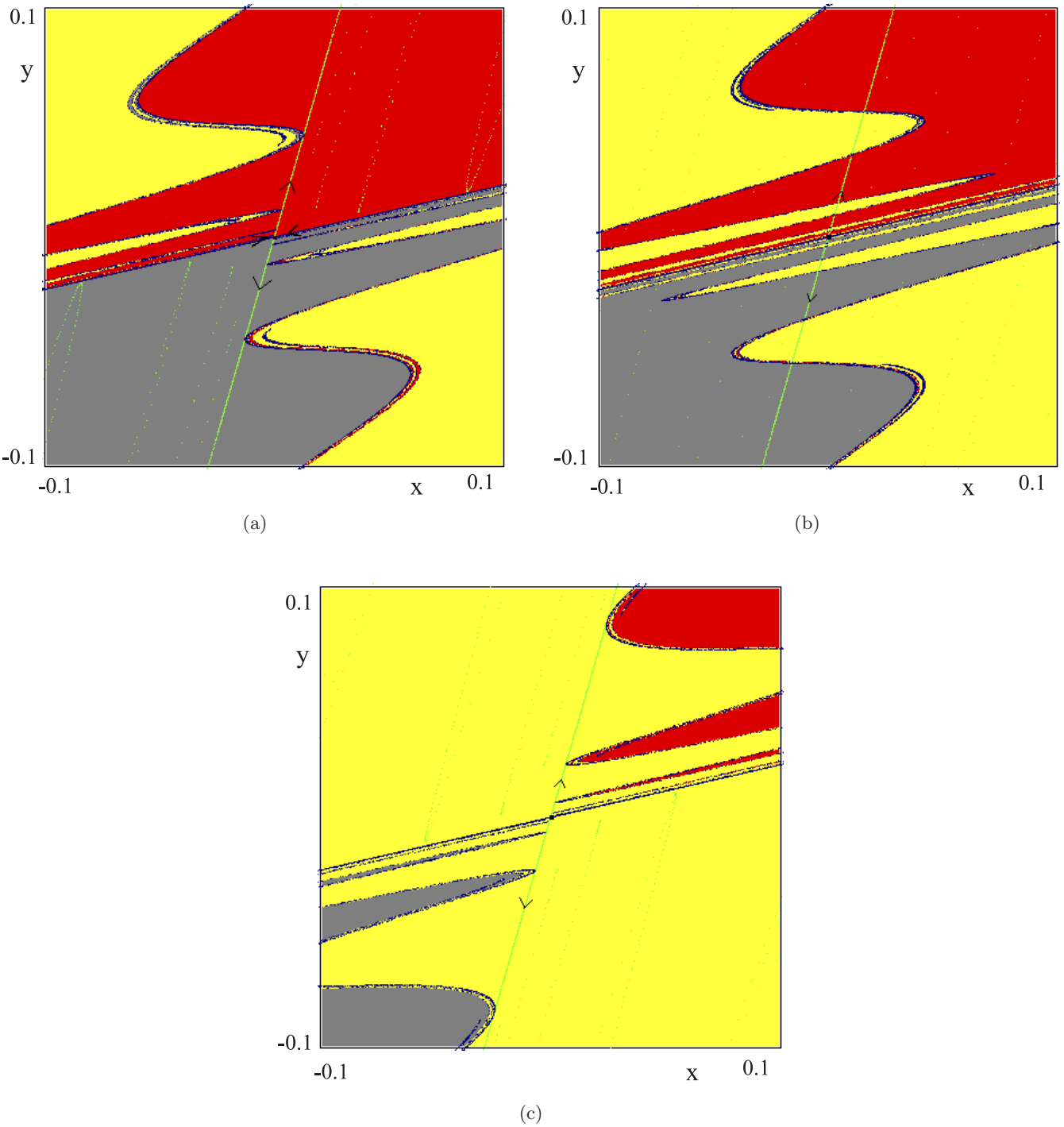

Fig. 13. (a) $b = -0.791468$, enlargement of a portion of Fig. 12. (b) $b = -0.7918$, the homoclinic tangle develops. (c) $b = -0.79283$, the tangency on the other side occurs.

Figure 16 presents a similar situation at a lower value of b. Differently from the case of Fig. 15, we no longer have the basins of the fixed points Q_i, because in that range of b the repelling closed invariant curves at the boundary of the two basins $B(Q_i)$ shrank and collapsed into the two fixed points through a subcritical Neimark bifurcation, after which Q_i are two repelling focuses. In Fig. 16(a) the stable and unstable sets $W^S(S_6)$ and $W^U(S_6)$ are represented by blue and green curves respectively. This figure shows that $W^S(S_6)$ and $W^U(S_6)$ are quite close, and this suggests that the bifurcation described in Fig. 5 is going to occur. The enlargement of Fig. 16(b), where the 6

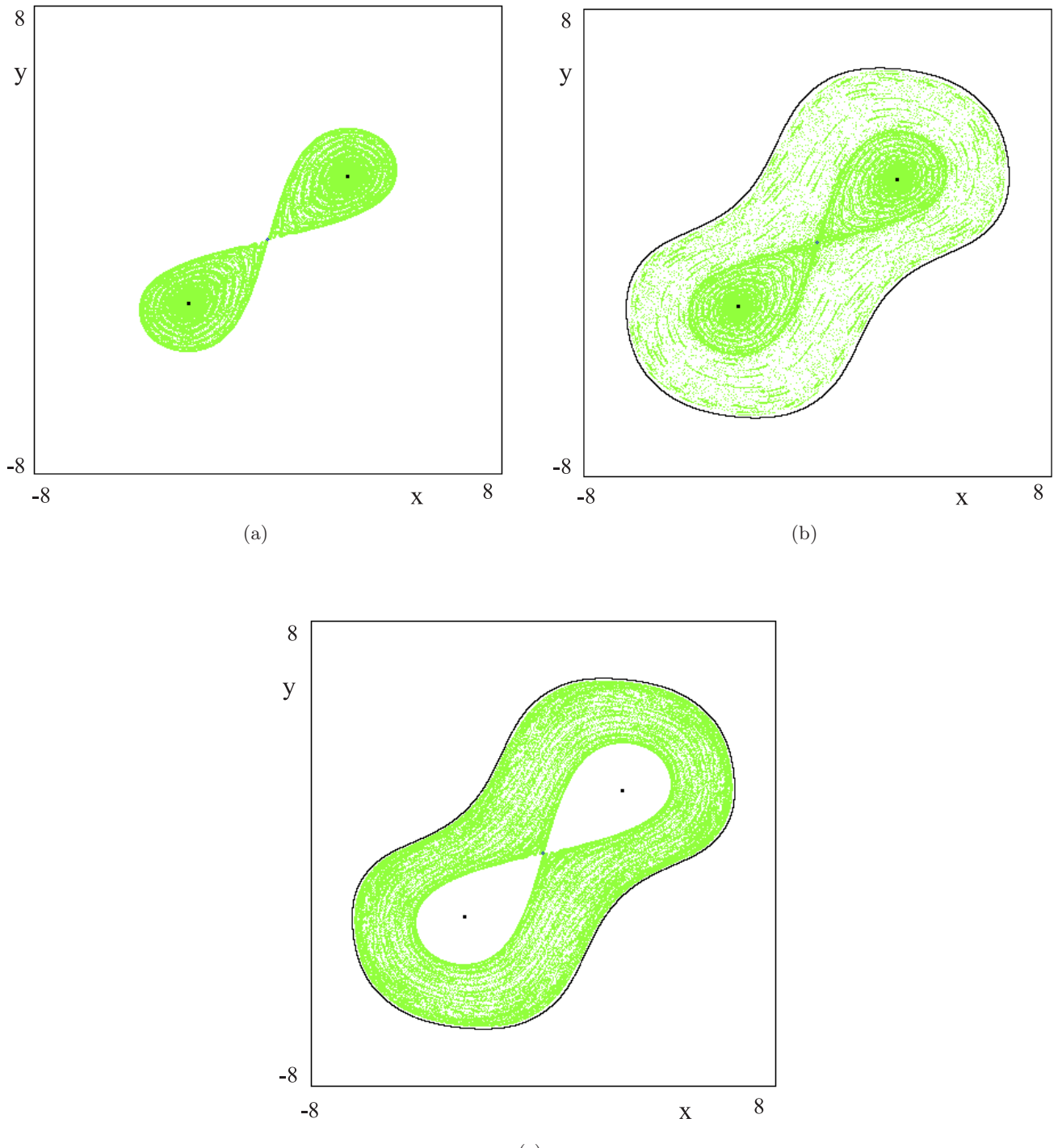

Fig. 14. The whole picture of $W^U(O)$. (a) $b = -0.791468$, (b) $b = -0.7918$, (c) $b = -0.79283$, i.e. the same set of parameters as in Figs. 13(a)–13(c), respectively.

basins of the stable fixed points $C_{6,i}$ of map T^6 are represented during the homoclinic tangle by different colors, $W_2^U(S_6) \cap W_2^S(S_6) \neq \emptyset$ [see Fig. 16(c)]. During the tangle the closed heteroclinic connection of the 6-cycle no longer exists, and the 6 basins of the map T^6 are intermingled in the outer part of the cycle. In Fig. 16(b) two more attracting cycles exists: a cycle C_{40} (yellow basin) and a cycle C_{23} (black basin). Figure 16(d) shows, after a very small change of b, that we are close to the second tangency between $W_2^U(S_6)$ and $W_2^S(S_6)$, after which another attracting closed invariant curve will appear outside

the cycle C_6, as shown in Fig. 17(a), where the 6-cycles no longer give an heteroclinic connection, whereas an attracting curve Γ exists outside that cycle, with a yellow basin.

From Fig. 17, we see the basin of a pair of cycles of period 5 (red and violet regions, respectively), that appeared via saddle-node bifurcations, outside Γ. We recall that the map T considered in this section is symmetric, hence a cycle of odd period cannot exist alone, as also a symmetric one must exist. In the case shown in Fig. 17(a) the basins of the two 5-cycles, say C_5 and C_5', are bounded

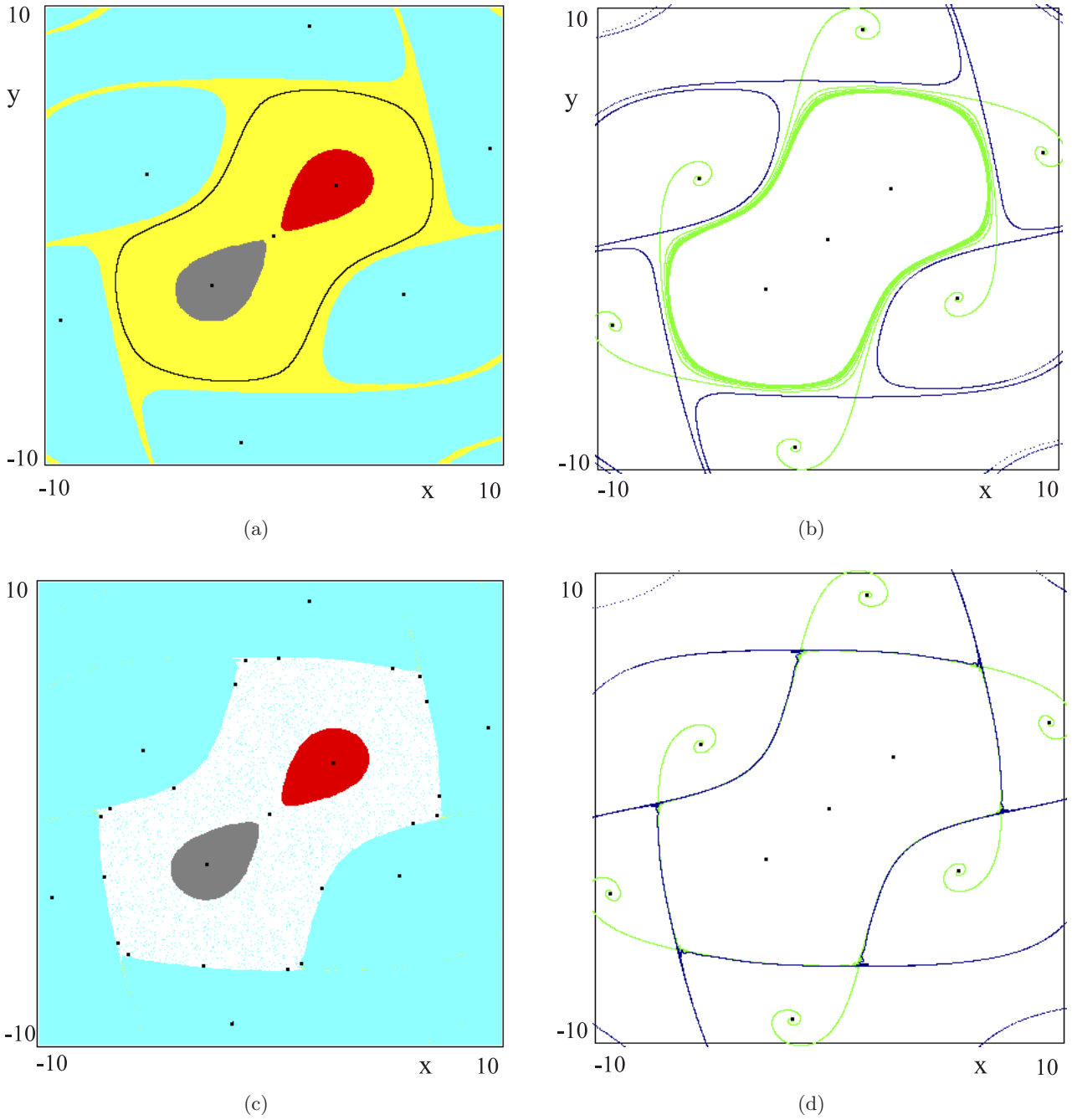

Fig. 15. (a) $b = -0.8$, basins and the attractors. (b) For the same set of parameters as in figure (a) $W_1^U(S_6)$ and $W_1^S(S_6)$ are represented in green and blue, respectively. (c) $b = -0.8071$, basins and the attractors. (d) For the same set of parameters as in figure (b) $W_1^U(S_6)$ and $W_1^S(S_6)$ are represented in green and blue, respectively. (e) Enlargement of a portion of figure (c). (f) Enlargement of a portion of figure (d). (g) $b = -0.8$, different colors are used to represent basins of the fixed points of the map T^6, separated by $W^S(S_6)$. (h) For the same set of parameters as in figure (g) $W_1^U(S_6)$ and $W_1^S(S_6)$ are represented in green and blue, respectively.

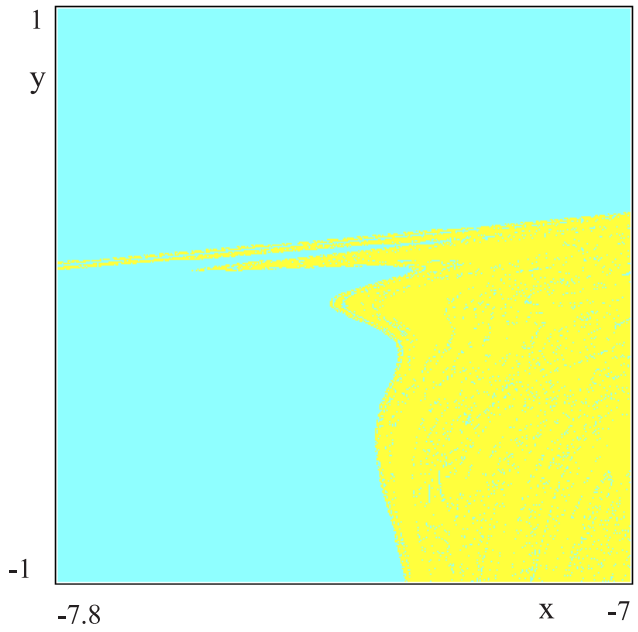

(e)

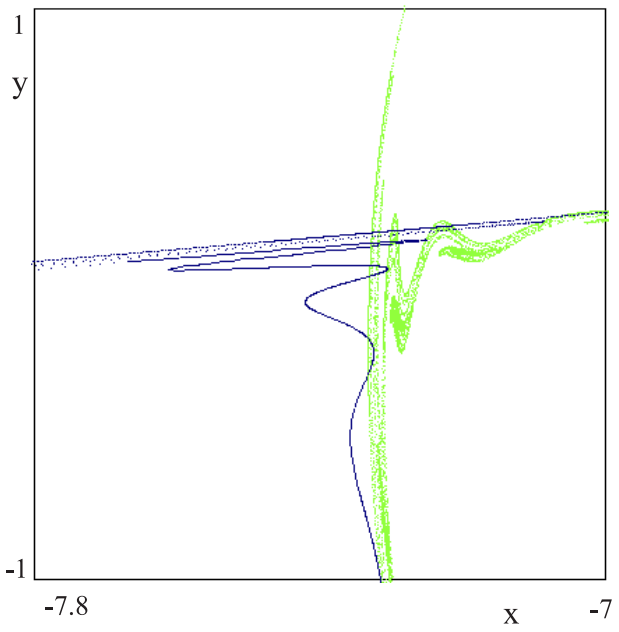

(f)

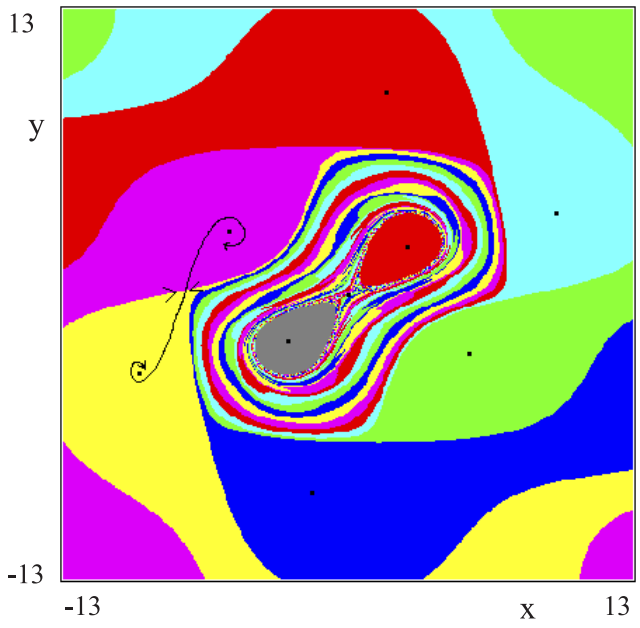

(g)

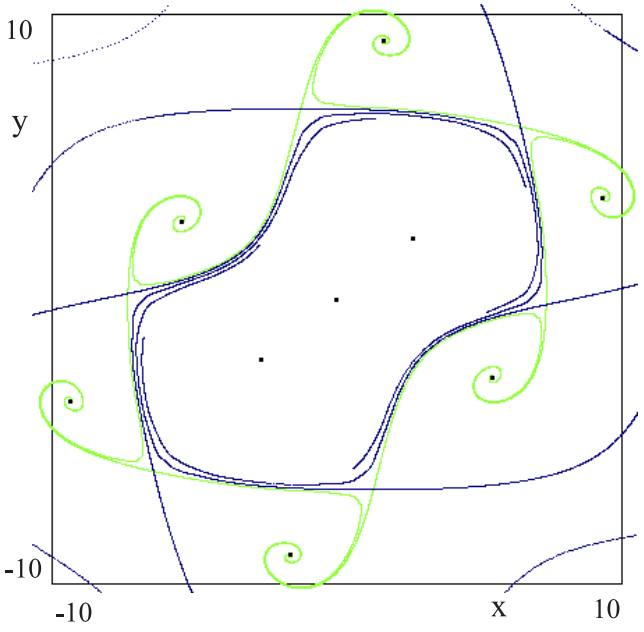

(h)

Fig. 15. (*Continued*)

by the stable sets of their related saddles, $W^S(S_5)$ and $W^S(S_5')$, while the two unstable branches have different limit sets.

In Fig. 17(a) we are again in the situation qualitatively described in Fig. 4(a), and the two tangles (of Figs. 4 and 5) are going to occur again by decreasing b, as we have just seen in relation with the cycle C_6. Figure 17(b) shows the basins at a lower value of b, evidencing that $W_1^U(S_5)$ and $W_1^S(S_5')$ are approaching to each other, and also the attracting curve Γ is approaching the stable set $W_1^S(S_5 \cup S_5')$ of the saddle. It is worth noting that even if we have two disjoint cycles of period 5, both are involved in giving a unique attracting closed invariant curve, that is a saddle-node or a saddle focus heteroclinic connection, as qualitatively

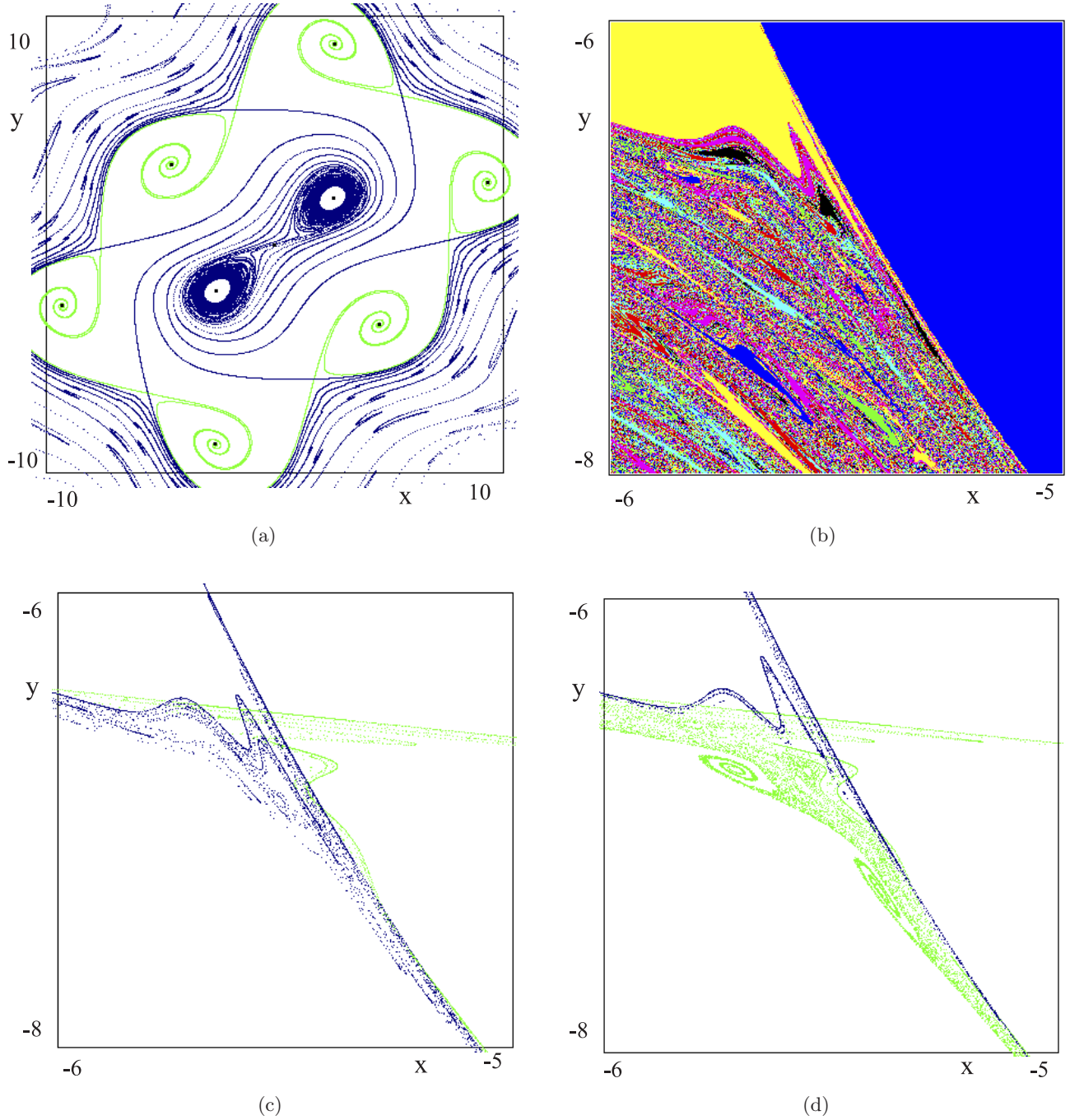

Fig. 16. (a) $b = -0.87$, $W_1^U(S_6)$ and $W_1^S(S_6)$ are represented in green and blue, respectively. (b) $b = -0.8711$, enlargement of the 6 basins of the stable fixed points $C_{6,i}$ of map T^6 during the homoclinic tangle. (c) $b = -0.8711$, as in figure (c), $W_2^U(S_6)$ and $W_2^S(S_6)$ are represented in green and blue, respectively. (d) $b = -0.8712$, $W_2^U(S_6)$ and $W_2^S(S_6)$ are represented in green and blue, respectively.

shown in Fig. 18, where the period of the two cycles has been taken equal to 3 in order to simplify the picture. The first homoclinic tangle appears after a small decrease of b with respect to the value used to get Fig. 17(b), and it is clearly visible in Fig. 17(c) and in its enlargement, Fig. 17(d) (we are in the situation qualitatively represented in Fig. 4(e)). Just after the homoclinic tangency (on the other side) of the two manifolds $W_1^U(S_5)$ and $W_1^S(S_5')$, the attracting curve Γ no longer exists whereas a saddle-focus connection between the cycles S_5, S_5', C_5 and C_5' exists, as evidenced in Fig. 19(a) (the unstable branches of S_5 and S_5' reach the cycles C_5 and C_5', as qualitatively shown in Fig. 18(b)).

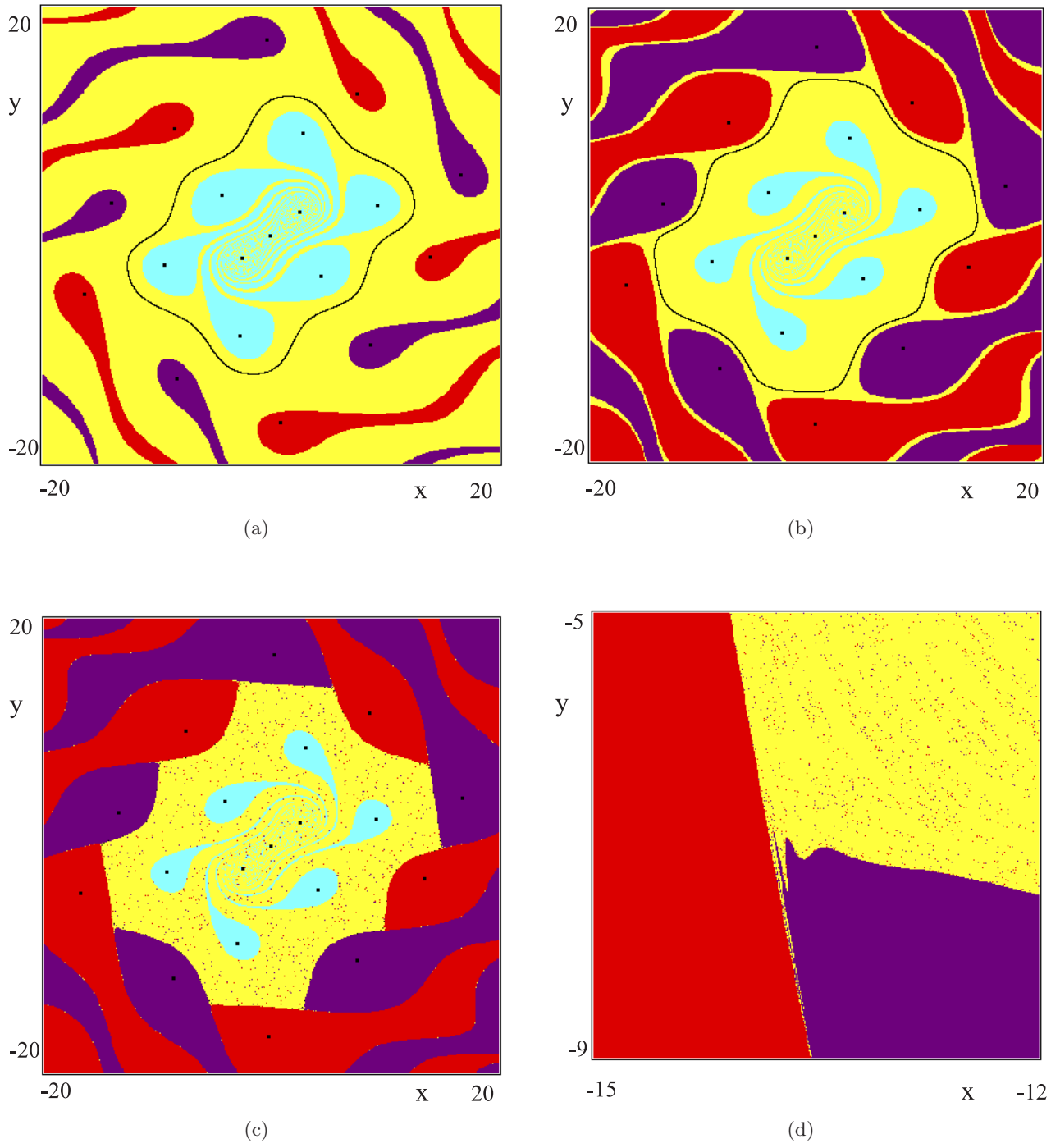

Fig. 17. Basins of four coexisting attractors. (a) $b = -0.88$ (b) $b = -0.895$ (c) $b = -0.8987$. (d) Enlargement of a portion of figure (c).

Figure 19(b) shows that the manifolds $W_2^U(S_5)$ and $W_2^S(S_5')$ are close to each other and the second homoclinic tangle (qualitatively described in Fig. 5) is going to occur, giving rise to a wider attracting closed invariant curve Γ, clearly visible in Fig. 19(c), with the two cycles C_5 and C_5' inside it, whose basins are separated by the stable set of the saddles S_5 and S_5', and the two branches of the unstable sets have different limit sets: the cycle and Γ. In that figure we also see the 6-cycle C_6 still attracting, and its basin of attraction is bounded by the stable set of the saddle S_6. The yellow region denotes the basin of Γ, and in that region another cycle is going to appear as b decreases. In fact, in

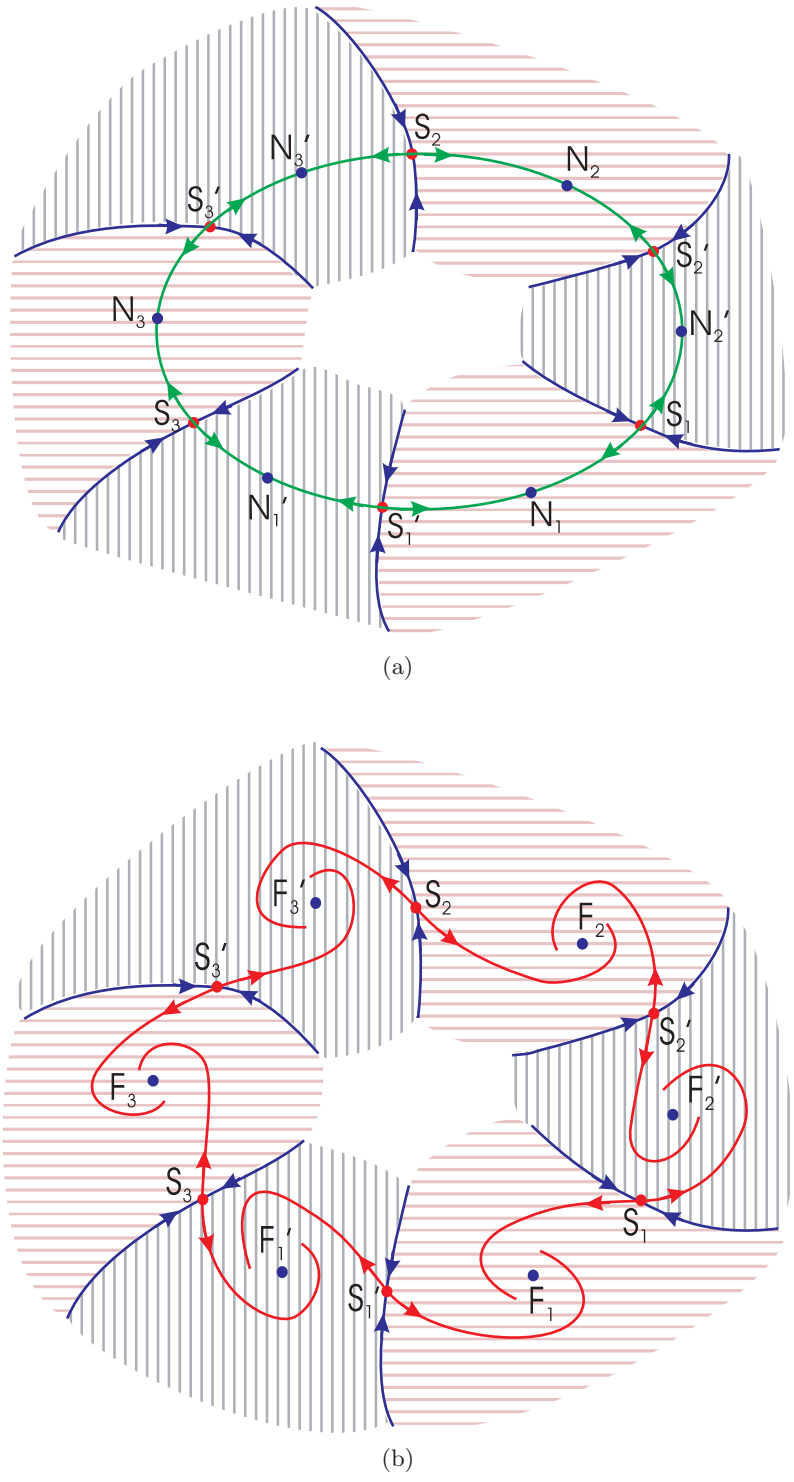

Fig. 18. Qualitative representation of (a) a saddle-node heteroclinic connection, (b) a saddle-focus heteroclinic connection.

Fig. 20(a) we see an attracting cycle C_{14} born by saddle-node bifurcation, whose basin (in green) is bounded by the stable set of the saddle S_{14}, and whose unstable branches have different limit sets: the cycle and Γ. We also note that in this last interval of b-values another homoclinic bifurcation of the 6-cycle S_6 has occurred, with the merging (or homoclinic tangle) of the branches $W_2^S(S_6)$ and $W_1^U(S_6)$ giving rise to 6 repelling closed invariant curves which bound the 6 basins of the periodic points $C_{6,i}$, as shown in the enlargement of that figure [Fig. 20(b)].

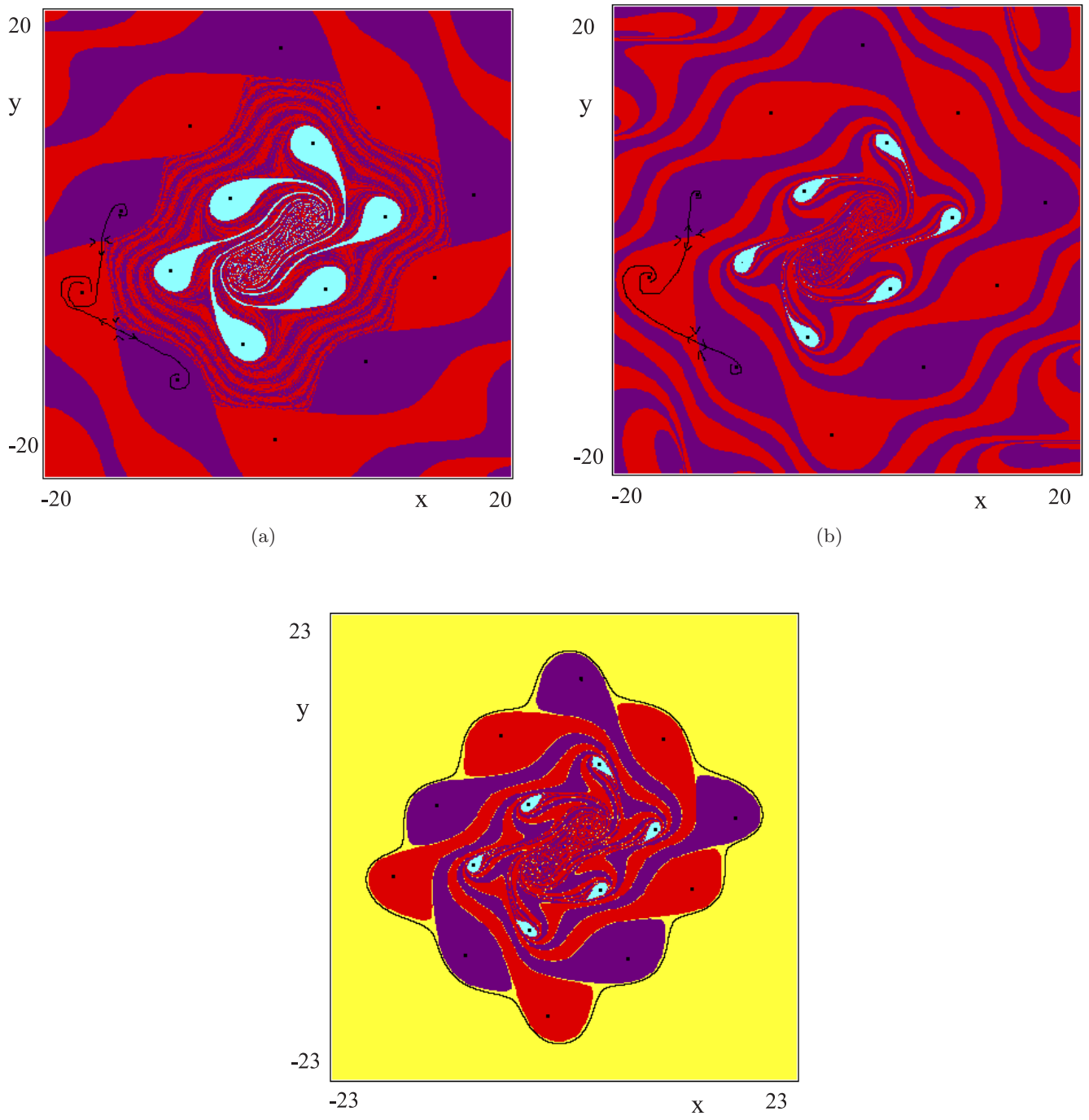

Fig. 19. (a) $b = -0.898$, a saddle-focus connection between the cycles S_5, S_5', C_5 and C_5' exists. (b) $b = -0.92$, the second homoclinic tangle (qualitatively described in Fig. 5) is going to occur. (c) $b = -0.925$, an attracting closed invariant curve Γ has been created, whose basin is represented by the yellow region.

Clearly, on further decreasing b, the basins of the 14-cycle will increase, the two manifolds $W_1^U(S_{14})$ and $W_1^S(S_{14})$ will approach each other and also the closed attracting curve Γ will approach such manifolds, and the homoclinic tangles will occur, first with $W_1^U(S_{14}) \cap W_1^S(S_{14}) \neq \emptyset$ and then with $W_2^U(S_{14}) \cap W_2^S(S_{14}) \neq \emptyset$, creating a wider closed invariant curve outside, and so on... the process is repeated several times.

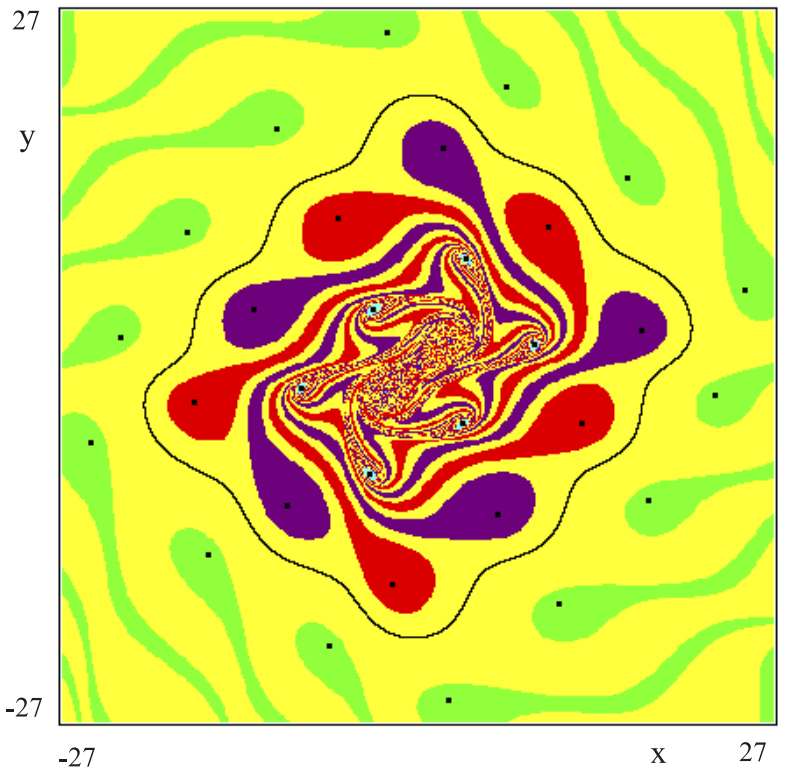

(a)

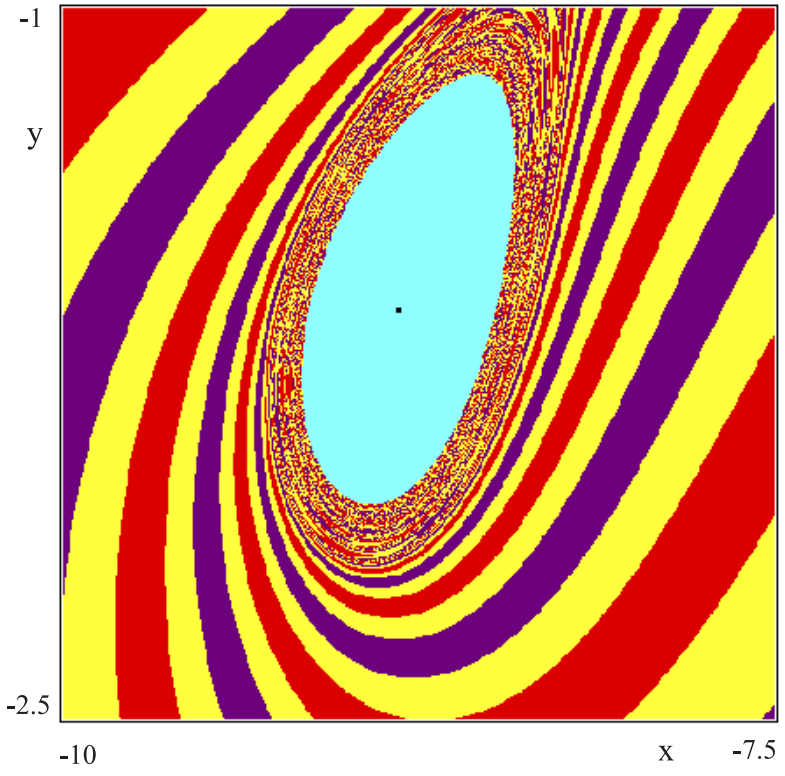

(b)

Fig. 20. (a) $b = -0.93$, an attracting cycle C_{14} exists, whose basin is represented in green. The yellow region represents the basin of the attracting closed curve Γ, and the other colors represent the basins of stable cycles of period 6. (b) Enlargement of a portion of figure (a).

4. A Family of Asymmetric Maps

In order to prove that the bifurcations described qualitatively in Sec. 2 and shown by the numerical examples of Sec. 3 are not related to some symmetry property of the map (1), in this section we shall consider the following nonsymmetric perturbation of the map (1):

$$T:\begin{cases} x' = ax + y \\ y' = \begin{cases} bx + cy + d\cdot\arctan y & \text{if } y \geq 0 \\ bx + cy + \dfrac{d}{\beta}\cdot\arctan(\beta y) & \text{if } y \leq 0 \end{cases} \end{cases} \tag{6}$$

where we assume $0 < a < 1$, $d > 0$ and $\beta > 0$. Again, T has a fixed point in the origin O, and two more fixed points exist, say again Q_1 and Q_2, if the parameters satisfy the condition given in (2), the only difference being that now the y-coordinate of the fixed point Q_1, located in the half-plane $y>0$, is the positive solution of the equation $my - \arctan y = 0$, while the y-coordinate of the fixed point Q_2, located in the half-plane $y < 0$, is the negative solution of the equation $my - \arctan(\beta y)/\beta = 0$. Now Q_1 and Q_2 are no longer in symmetric positions with respect to O.

The Jacobian matrix of T is

$$DT(x,y) = \begin{cases} \begin{bmatrix} a & 1 \\ b & c + \dfrac{d}{1+y^2} \end{bmatrix}, & \text{for } y \geq 0 \\ \begin{bmatrix} a & 1 \\ b & c + \dfrac{d}{1+\beta^2 y^2} \end{bmatrix}, & \text{for } y \leq 0 \end{cases}$$

and it becomes identical to the matrix in (3a) when computed in the basic fixed point O. Thus the stability region of O is the same as the one determined in Sec. 3 [see Fig. 7(a)].

As the Jacobian determinant is given by

$$\det DT = \begin{cases} (ac-b) + \dfrac{ad}{1+y^2} & y \geq 0 \\ (ac-b) + \dfrac{ad}{1+\beta^2 y^2} & y \leq 0 \end{cases}$$

it vanishes on two straight lines of the plane (one in the half-plane $y > 0$, and one in the half-plane $y < 0$) of equation

$$y = \sqrt{\frac{ad}{b-ac} - 1}$$

$$y = -\frac{1}{\beta}\sqrt{\frac{ad}{b-ac} - 1}$$

if the condition (5) holds. Thus, also in this case, when the parameters are taken in the strip $ac < b < ac + ad$ of the (c, b) parameter plane, then map T is noninvertible, of type $Z_1 - Z_3$. However, the parameter values used in the following always belong to the region in which T is invertible. In fact, we fix the parameters $a = 0.2$, $c = -0.1$, $d = 4$ and $\beta = 2$, while b is decreased, starting from values close to the pitchfork bifurcation curve, where we have the two stable fixed points Q_i, each with its own basin of attraction. This is the situation shown in Fig. 21(a), where the two basins $B(Q_i)$ (gray and red regions) are separated by $W^S(O)$ (blue lines) while the two branches of $W^U(O)$ (green lines) tend to the attracting fixed points Q_i.

4.1. *Appearance of cycles and of closed invariant curves*

On decreasing the parameter b, several cycles appear. In Fig. 21(b) we show, besides the two basins $B(Q_i)$, separated by $W^S(O)$, the basin of a 6-cycle C_6 (pale blue region) bounded by the stable set $W^S(S_6)$ of the saddle S_6 born with C_6. As b is further decreased, other cycles appear, again via saddle-node bifurcations: a pair of 8-cycles, a pair of 9-cycles and a pair of 10-cycles. In Fig. 21(c) the basins of the stable cycles are represented by different colors: $B(Q_i)$ in red and gray, $B(C_6)$ in pale blue, $B(C_8)$ in green, $B(C_9)$ in violet, $B(C_{10})$ in dark blue, see also the enlargement in Fig. 21(d). No closed invariant curves exist, and the two branches of the unstable set have different attractors as limit sets. In the enlargement we can see that the inner branches of the saddle S_{10} are close to each other, and that the tongues of the basins $B(Q_i)$ are very thin and close to the stable set $W^S(S_{10})$. In fact, we are close to the bifurcation qualitatively described in Fig. 2: as b is further decreased, $W_1^U(S_{10})$ and $W_1^S(S_{10})$ merge and switch, giving rise to an inner repelling closed invariant curve $\tilde{\Gamma}$ (limit set of $W^S(O)$) and a closed invariant attracting curve is created by the saddle-focus heteroclinic connection

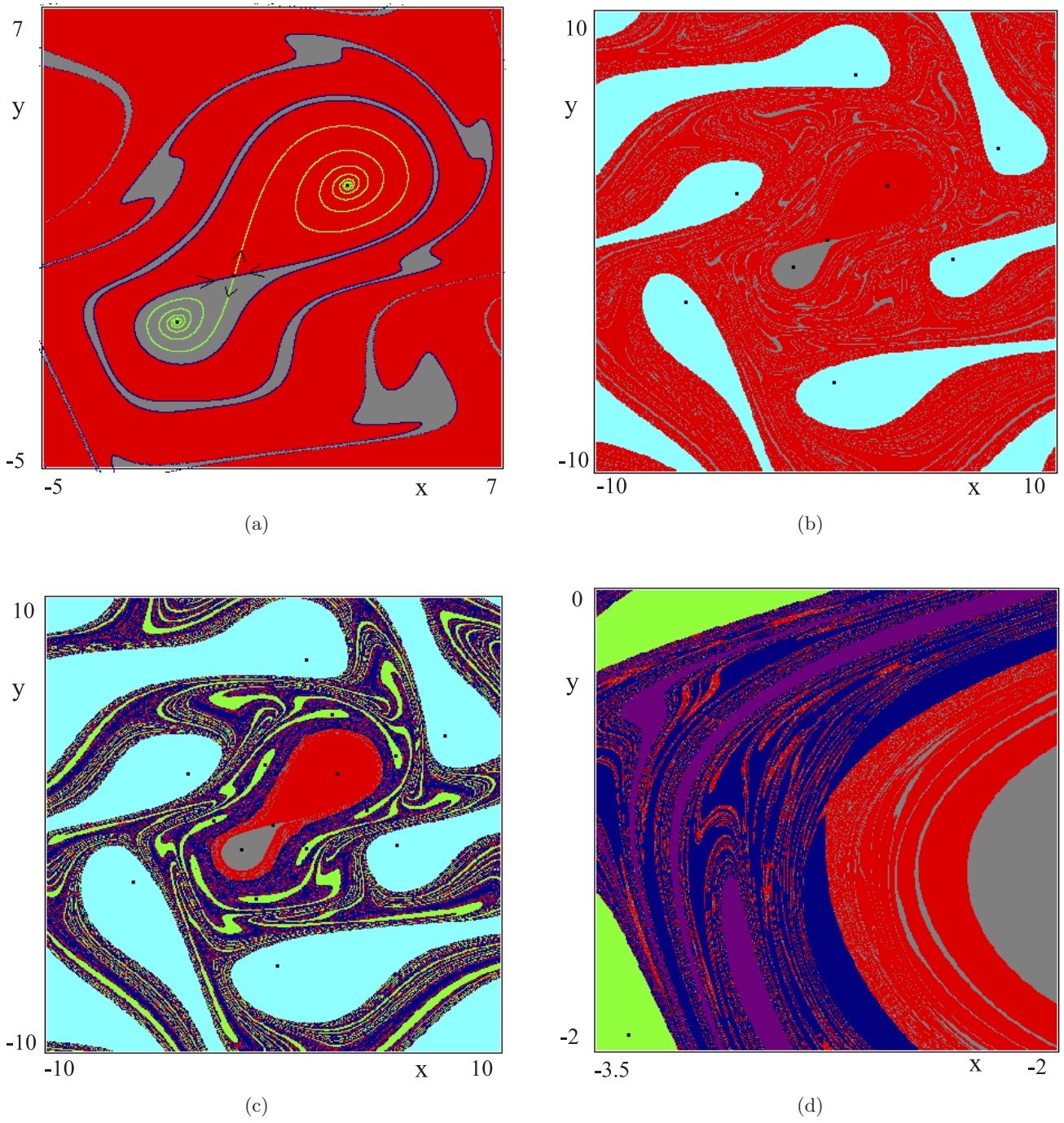

Fig. 21. Asymmetric map (6), we fix the parameters $a = 0.2$, $c = -0.1$, $d = 4$ and $\beta = 2$. (a) For $b = -0.7$ the basins of the two stable fixed points Q_i are represented by gray and red regions, separated by the stable set $W^S(O)$ of $O = (0, 0)$ (blue curves), whereas the two branches of $W^U(O)$ (green curves) tend to the attracting fixed points Q_i. (b) $b = -0.76$, a 6-cycle C_6 also exists, whose basin is the pale blue region. (c) $b = -0.76775$, also a stable 8-cycle C_8, a stable 9-cycle C_9 and a stable 10-cycle C_{10} exist, whose basins are represented by different colors: $B(C_8)$ in green, $B(C_9)$ in violet, $B(C_{10})$ in dark blue. (d) Enlargement of a portion of figure (c).

of the two cycles S_{10} and C_{10}. This situation is shown in the enlargement of Fig. 22(a). However, we are already close to the second homoclinic tangle represented in the qualitative Fig. 5, which will be followed by the bifurcation described in Fig. 6, In fact, homoclinic points of the second homoclinic tangle, due to $W_2^U(S_{10}) \cap W_2^S(S_{10}) \neq \emptyset$, are visible in Fig. 22(b), where the yellow points converge

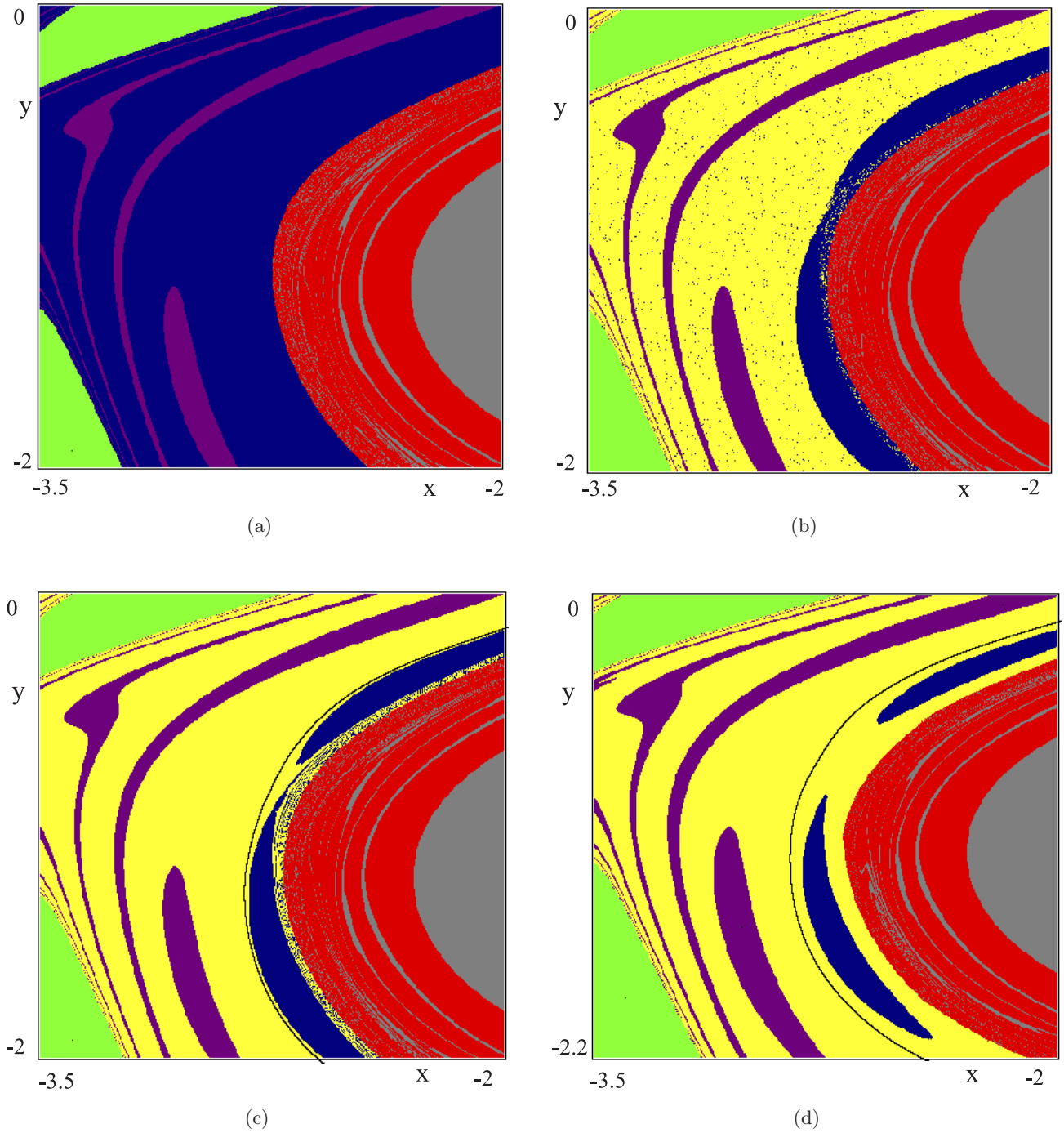

Fig. 22. (a) $b = -0.7678$. Enlargement of the basins $B(C_8)$ in green, $B(C_9)$ in violet, $B(C_{10})$, $B(Q_1)$ in gray, $B(Q_2)$ in red. (b) $b = -0.76785$, the bifurcation qualitatively described in Fig. 2 is going to occur, the yellow region represents the basin of attraction of a stable cycle of high period that exists during the homoclinic tangle. (c) $W_1^U(S_{10})$ and $W_1^S(S_{10})$ merge and switch, giving rise to an inner repelling closed invariant curve $\tilde{\Gamma}$ and a closed invariant attracting curve Γ, whose basin is represented by the yellow region. (d) $b = -0.76807$, after the bifurcation 10 repelling closed invariant curves are created, which bound the basins of the stable focuses $C_{10,i}$ (dark blue).

to an attracting cycle existing during the tangle. In Fig. 22(c), obtained just after the tangency, a new attracting closed invariant curve Γ exists outside the invariant manifolds of the 10-cycles. Its basin is represented by the yellow region. The 10-cycles belong to the strip bounded by the two closed curves Γ (attracting) and $\tilde{\Gamma}$ (repelling). $\tilde{\Gamma}$ bounds on one side the basin $B(\Gamma)$ (yellow) and is also the

limit set of the basin $B(C_{10})$ (dark blue), while on the other side it is the limit set of the two basins $B(Q_i)$ (gray and red). Inside the strip bounded by Γ and $\tilde{\Gamma}$ the basin $B(C_{10})$ is made up of 10 disjoint sectors, each one bounded by the stable set $W^S(S_{10,i})$ for $i = 1, \ldots, 10$. The unstable branch $W_1^U(S_{10})$ tends to the attracting focus C_{10} while the unstable branch $W_2^U(S_{10})$ tends to the closed curve Γ. However, on decreasing the parameter b, we observe that $W_1^U(S_{10})$ approaches $W_2^S(S_{10})$, and the homoclinic loop qualitatively described in Fig. 6 occurs, probably via an homoclinic tangle. The result, after the bifurcation, is that 10 repelling closed invariant curves are created, which bound the basins of the stable focuses $C_{10,i}$ (dark blue) as shown in the enlargement of Fig. 22(d). These closed repelling curves will decrease in size as b decreases and will merge with the cycle via a subcritical Neimark bifurcation creating a repelling focus C_{10}.

In Fig. 23(a) we show the situation at a lower value of the parameter: the 10-cycles (a saddle and a repelling focus) merged with the closed repelling invariant curve $\tilde{\Gamma}$ giving rise to a repelling saddle-focus invariant curve, that bound the basins of the stable fixed points Q_i on one side (red and gray points) and the basin $B(\Gamma)$ on the other side (yellow). In the enlargement shown in Fig. 23(b), we can also see that the basin $B(\Gamma)$ approaches $W_1^U(S_9)$, and $W_1^S(S_9)$ which are close to each other. This suggests that we are near the homoclinic tangle described in Fig. 4, which will destroy the attracting closed curve Γ, leaving a closed invariant curve made up of the saddle-focus connection of the 9-cycle, as shown in Fig. 23(c).

If we continue to decrease the parameter b, several homoclinic tangles of different cycles occurs, giving wider and wider closed invariant curves.

4.2. *Homoclinic bifurcation of the origin*

Continuing to decrease the parameter b, starting from the situation of Fig. 23, we can see that the repelling closed invariant curve $\tilde{\Gamma}$, which continues to be the limit set of the saddle O, shrinks near the origin (Fig. 24), and the homoclinic bifurcation of O (qualitatively described in Fig. 3) is going to occur. During the range of b in which the homoclinic tangle occurs, the wide picture of the basins

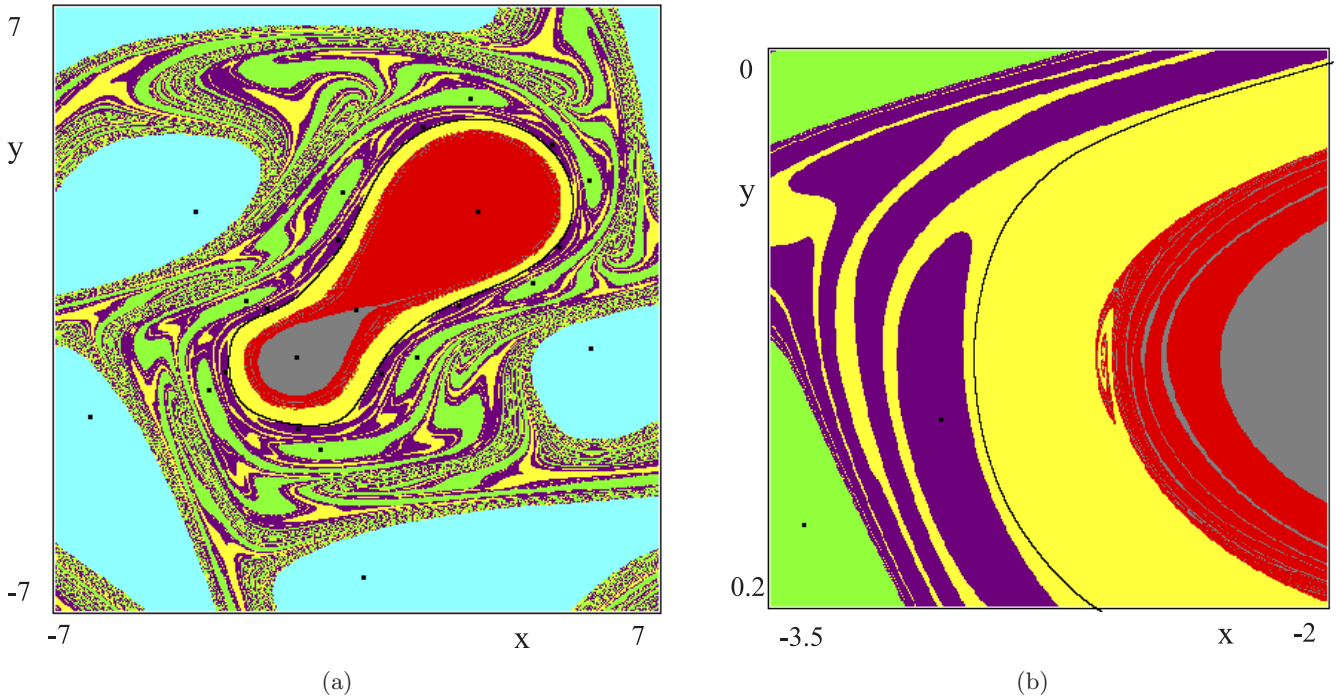

Fig. 23. (a) $b = -0.769$, a repelling saddle-focus invariant curve bounds the basins of the stable fixed points Q_i on one side (red and gray regions) and the basin $B(\Gamma)$ on the other side (yellow). (b) Enlargement of a portion of figure (a). (c) $b = -0.77$, the closed curve Γ no longer exists, and the violet region represents the basin of a closed invariant curve made up of the saddle-focus connection of a 9-cycle.

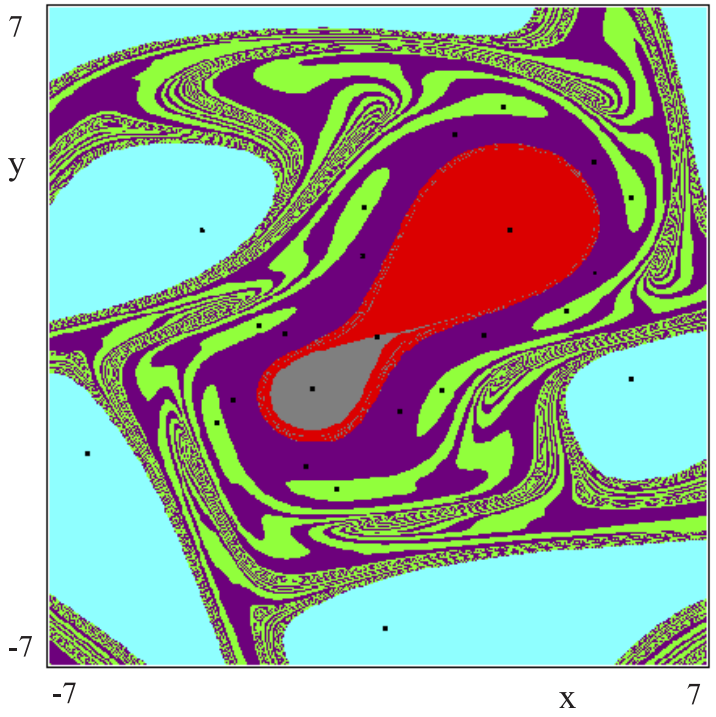

(c)

Fig. 23. (*Continued*)

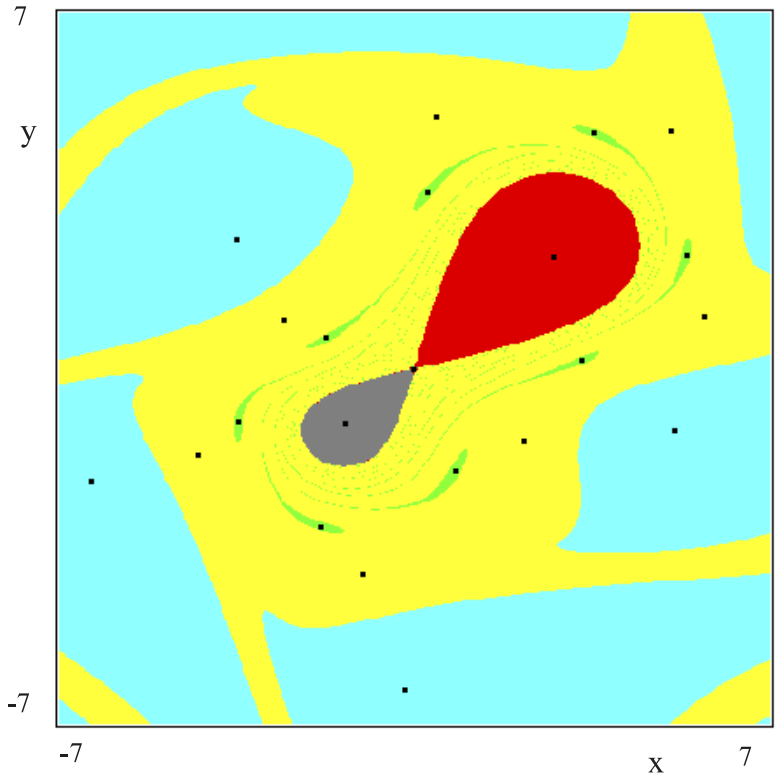

Fig. 24. $b = -0.79145$.

is always the same as that shown in Fig. 24 (at that scale): the attracting closed curve is formed by a saddle-focus heteroclinic connection of a 7-cycle (yellow basin) and the pair of 6-cycles still exists outside (the basin of the stable one is represented by the pale blue regions, bounded by the stable set $W^S(S_6)$). Instead, the pair of 8-cycles is inside the closed curve, with basin (green points) bounded by the stable set $W^S(S_8)$, while the two branches of $W^U(S_8)$ have different limit sets.

We show the dynamic behaviors of the stable and unstable sets of O in the enlargements of Figs. 25 and 26, where an homoclinic tangle is similar to the one observed in the previous section

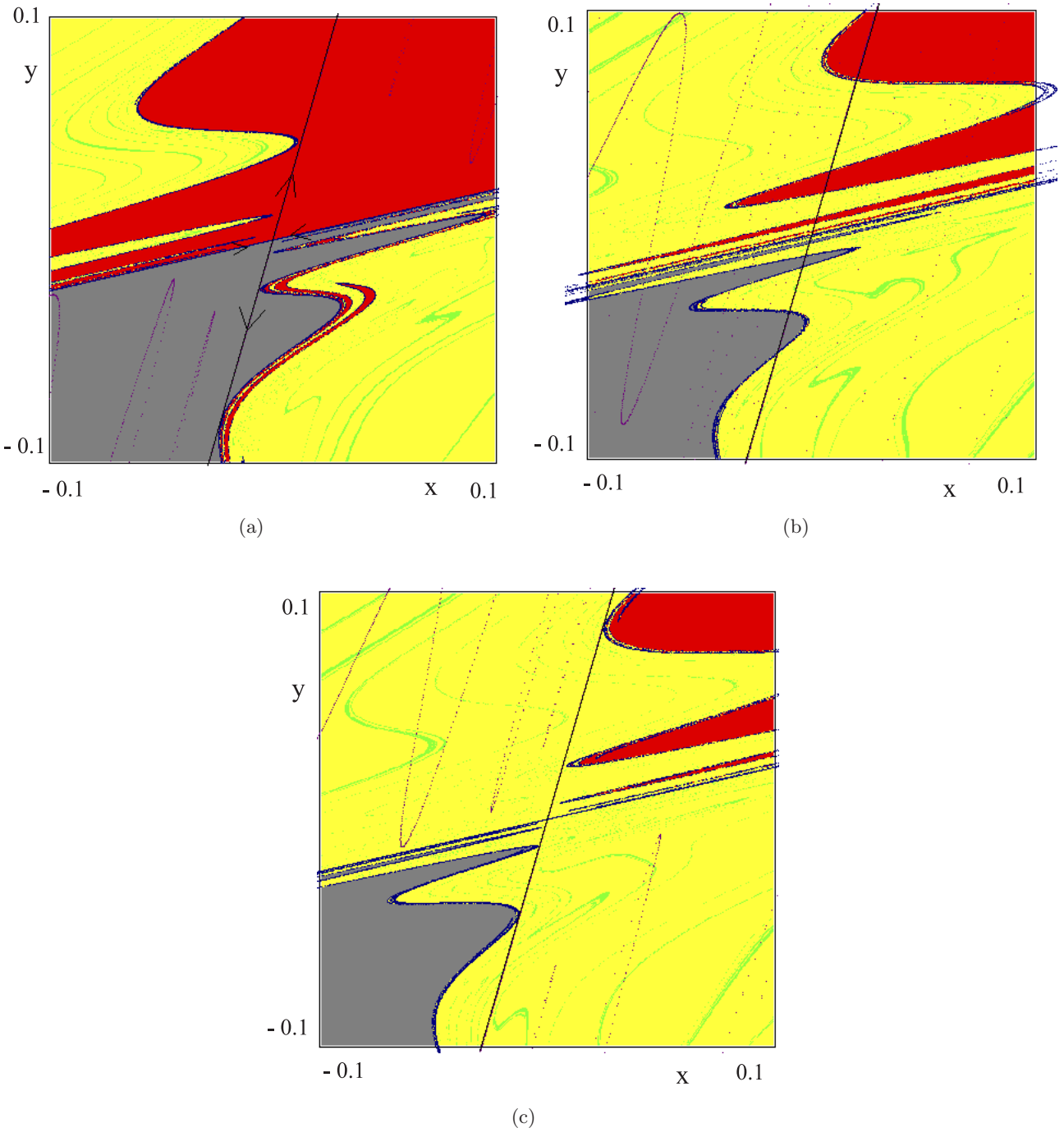

Fig. 25. Behavior of the stable set of O, $W^S(O)$ (blue) and its unstable set $W^U(O)$ (black) during the homoclinic tangle. (a) $b = -0.79145$, like in Fig. 24. (b) $b = -0.7925$. (c) $b = -0.792841$.

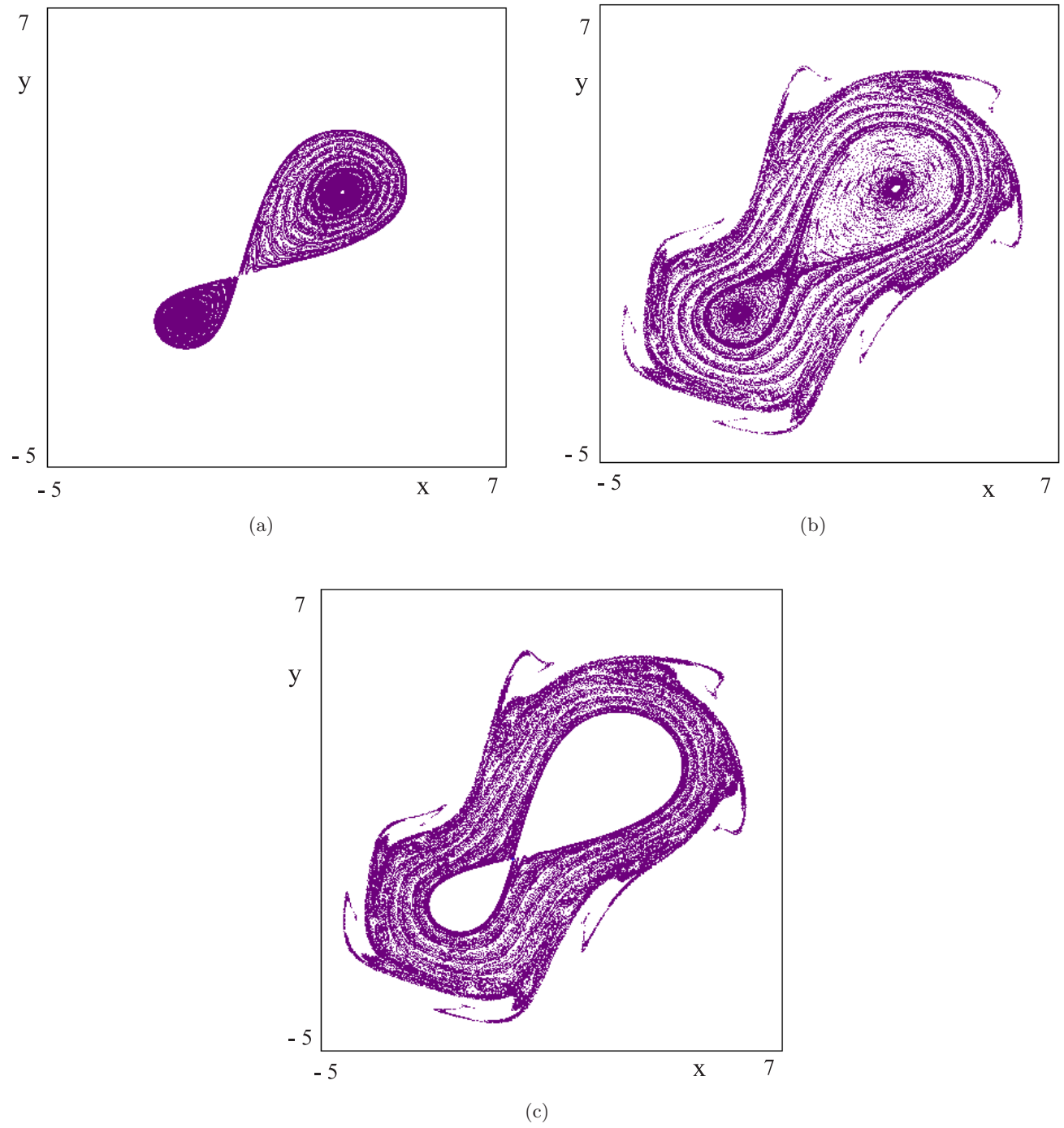

Fig. 26. The whole picture of $W^U(O)$. (a) $b = -0.79145$, (b) $b = -0.7925$, (c) $b = -0.792841$, i.e. the same set of parameters as in Figs. 25(a)–25(c) respectively.

for the symmetric map. In the enlargement of a neighborhood of the origin shown in Fig. 25(a) we can see the first homoclinic tangency between $W^U(O)$ (black line) and $W^S(O)$ (blue line). The whole branch of the unstable set visible on the right belongs to the red basin and tends to the fixed point Q_2, whereas the other branch belongs to the gray region and tends to the fixed point Q_1. Both are represented as a whole in Fig. 26(a), at the same parameter values as in Fig. 25(a). In Fig. 25(a) we can see that the stable set $W^S(O)$ has already a complex structure: the closed invariant

repelling curve $\tilde{\Gamma}$ is replaced by a strange repellor, which separates the two basins $B(Q_i)$ (gray and red) from $B(C_7)$ (yellow) and $B(C_6)$ (green). Figure 25(b) shows the transverse crossings between $W^S(O)$ and $W^U(O)$, which are homoclinic points of O. The stable set $W^S(O)$ still is the separator between the two basins $B(Q_i)$ and its limit set is a chaotic repellor. During the tangle, the unstable set of the origin, $W^U(O)$, includes segments of points belonging to $B(C_7)$ (yellow points) and $B(C_6)$ (green points) alternated with intervals of points belonging to the red and gray regions, and converging to the two fixed points. The whole picture of $W^U(O)$ at this set of parameter values is shown in Fig. 26(b).

The tongues of the two manifolds move on the other side with respect to the initial situation: more and more points of $W^U(O)$ belong to the yellow and green regions, and when the tangency on the other side occurs, as shown in Fig. 25(c), the whole unstable set of O tends to Γ, as shown in Fig. 26(c).

This closes the homoclinic tangle. After this tangency $W^U(O) \cap W^S(O) = \emptyset$, that is no homoclinic points of O survive, and with them also the chaotic repellor disappears, leaving two disjoint repelling closed invariant curves $\tilde{\Gamma}_i$ as basin boundaries of the fixed points Q_i (see Fig. 27). In Fig. 27 we also see that the 8-cycle has disappeared, the 7-cycle forms a closed invariant curve via a saddle-focus heteroclinic connection, and the 6-cycle has the inner stable and unstable manifolds which are approaching each other.

4.3. *Transitions with homoclinic tangles*

In Sec. 4.1 we have described several transitions from closed invariant curves to wider ones with several double homoclinic tangles (with the inner branches first and with the outer ones after), and many such situations occur for values of b ranging from the situation of Fig. 23 to that of Fig. 24. Usually the homoclinic tangles take place in a narrow interval of b-values. However, here we comment in detail one more transition because each step of the bifurcations qualitatively described in Fig. 4, with the homoclinic tangles both of the closed curve Γ (here represented by the saddle-focus connection of the 7-cycle in Fig. 27) and of the external saddle cycle (here the 6-cycle in Fig. 27), can be

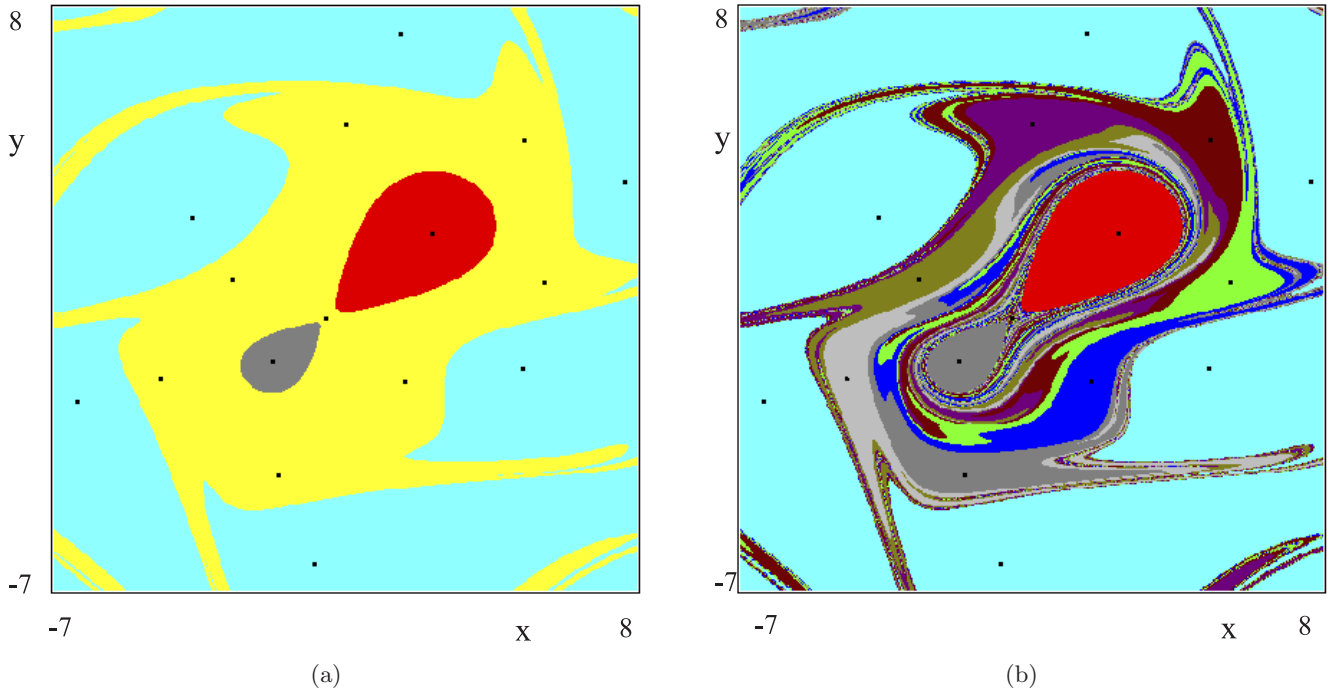

Fig. 27. (a) $b = -0.798$, basins of a 7-cycle C_7, yellow, a 6-cycle C_6, pale blue, the fixed points Q_1 and Q_2 (red and gray, respectively). (b) For the same set of parameters as in figure (a), seven different colors are used to represent basins of the fixed points $C_{7,i}$ of the map T^7, separated by $W^S(S_7)$. (c) Invariant manifolds $W^U(S_6)$ (violet) and $W^S(S_6)$ (blue). (d) Invariant manifolds $W^U(S_7)$ (violet) and $W^S(S_7)$ (blue).

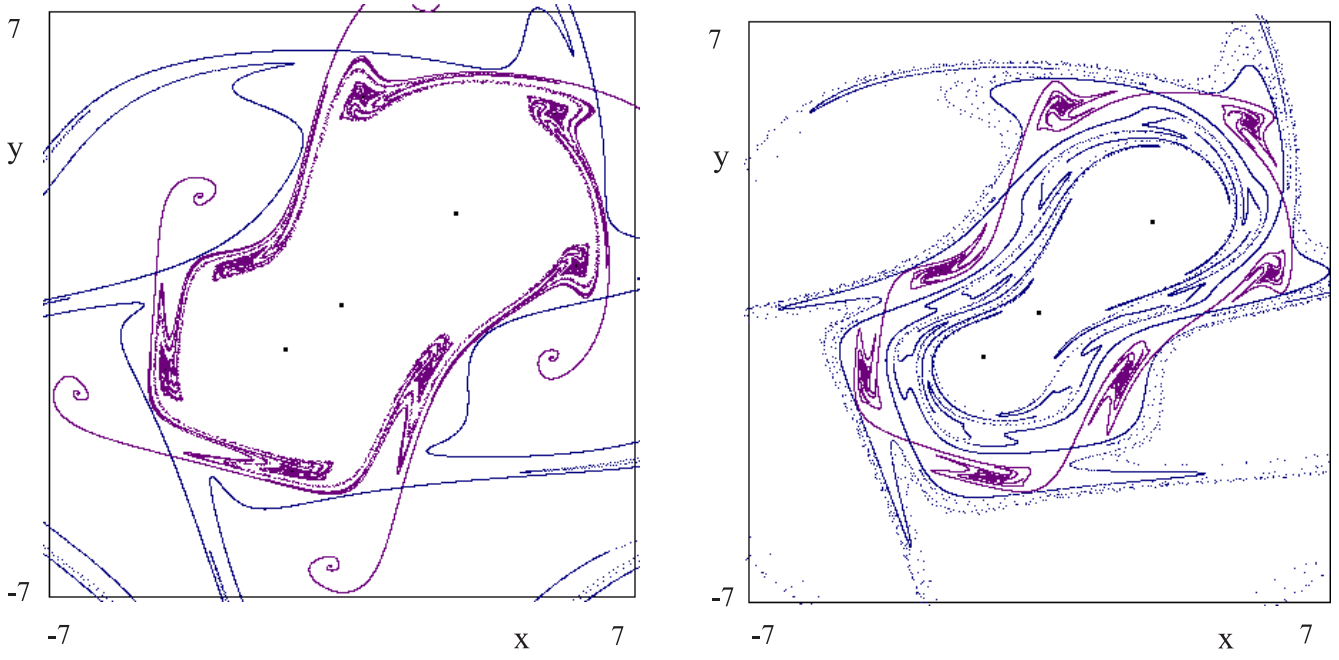

(c) (d)

Fig. 27. (*Continued*)

described in detail, as all of them occur in a wider range of b values. As already remarked in Sec. 2, it is possible that the homoclinic tangles associated with the closed curve Γ and the ones associated with the saddle cycle, involving the manifolds $W_1^U(S_q)$ and $W_1^S(S_q)$ require two different descriptions. This can be seen in this example, because the closed curve Γ is a simple saddle-focus connection of a 7-cycle. Figure 27(b) is performed at the same parameter value of Fig. 27(a), but using 7 different colors for the basins of the fixed points $C_{7,i}$, of T^7, bounded by the stable set $W^S(S_7)$. This suggests that the invariant manifolds $W^U(S_7)$ and $W^S(S_7)$, represented in Fig. 27(d), are close to an homoclinic tangency. Also the invariant manifolds $W^U(S_6)$ and $W^S(S_6)$, represented in Fig. 27(c), are approaching each other, but their homoclinic tangle will occur later. That is, we first observe an homoclinic tangle between two branches of the sets $W^U(S_7)$ and $W^S(S_7)$, causing the appearance of homoclinic points to S_7, thus causing the destruction of the closed invariant curve, even if the cycle C_7 persists in being attracting, as well as the cycle C_6. This is shown in Figs. 28(a) and 28(b), where we can deduce that the cycle S_6 is very close to its tangent homoclinic bifurcation, as clearly shown by the invariant manifolds $W^U(S_6)$ and $W^S(S_6)$ represented in Fig. 28, while the transverse crossing of the 7-cycle S_7 has already occurred, and homoclinic points of $W^U(S_7) \cap W^S(S_7)$ are clearly visible in Fig. 28(d). Figures 28(e) and 28(f), obtained with a lower value of b, show that now the manifolds $W_1^U(S_6)$ and $W_1^S(S_6)$ intersect transversely. At the parameter value of Figs. 28(e) and 28(f) and, after a further decrease of b, in Fig. 29, the basins $B(C_7)$ and $B(C_6)$ are quite intermingled, and we are within the homoclinic tangle of both cycles. Figure 29(a) shows the basin of C_7 (yellow), while 6 different colors are used for the basins of $C_{6,i}$, whose boundary is given by the stable set $W^S(S_6)$ shown, together with $W^U(S_6)$, in Fig. 29(b), where homoclinic points of S_6 are clearly visible, and homoclinic points of $W^U(S_7) \cap W^S(S_7)$ are shown in Fig. 29(c).

On decreasing b, the first tangency is one of 7-cycle, leaving 7 disjoint basins. However, the homoclinic points of the saddle cycle S_6 still exist, so that the basins of attraction are still intermingled with the basin of the 6-cycle C_6. Figure 30 shows the situation in this case: the yellow region represents the basin of C_7, while 6 different colors are used for the basins of $C_{6,i}$, considered as stable fixed points of T^6, whose boundary is given by the stable set $W^S(S_6)$. This is shown, together with $W^U(S_6)$, in

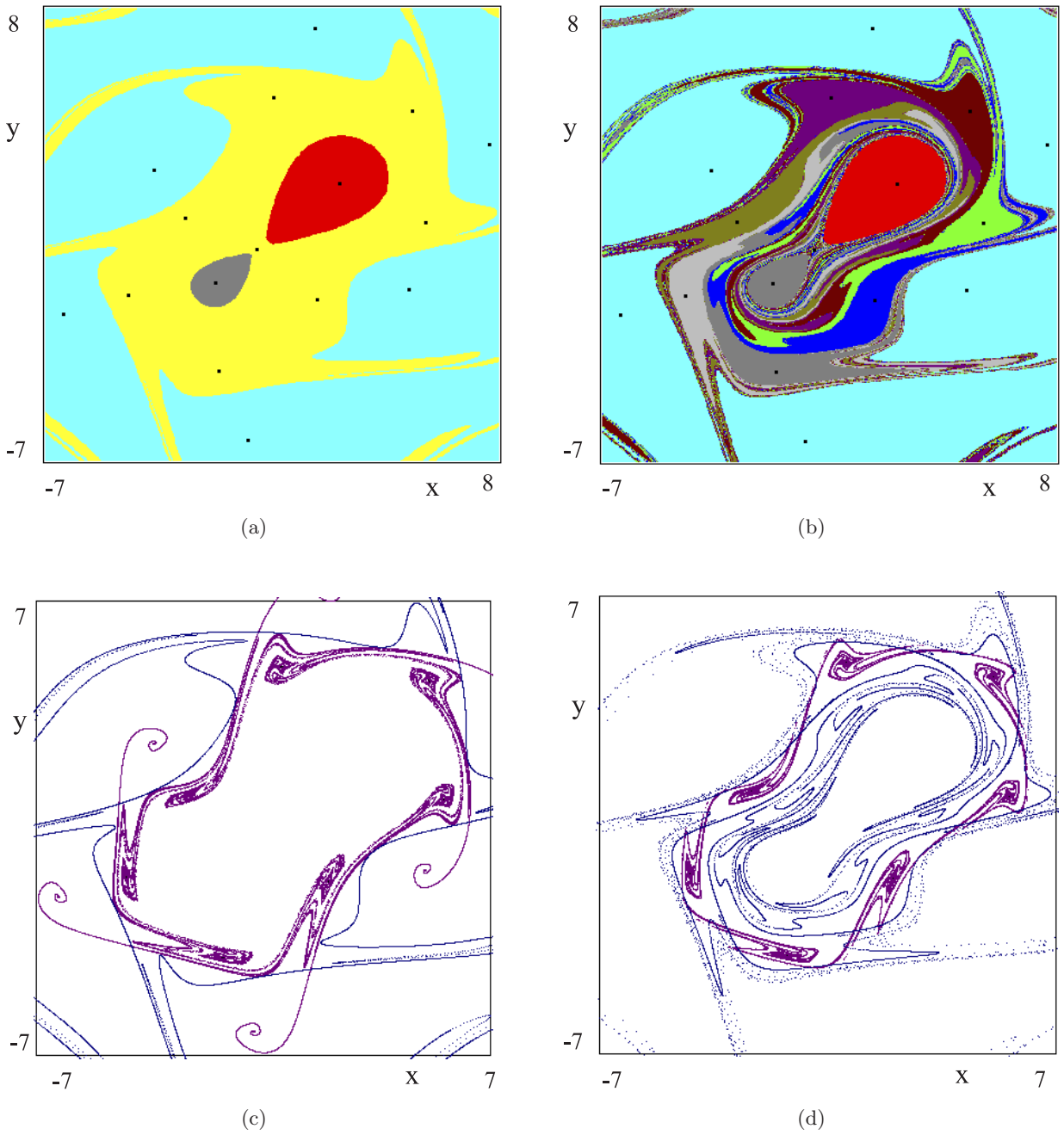

Fig. 28. (a) $b = -0.8$, basins of a 7-cycle C_7, yellow, a 6-cycle C_6, pale blue, the fixed points Q_1 and Q_2 (red and gray, respectively). (b) for the same set of parameters as in figure (a), seven different colors are used to represent basins of the fixed points $C_{7,i}$ of the map T^7, separated by $W^S(S_7)$. (c) Invariant manifolds $W^U(S_6)$ (violet) and $W^S(S_6)$ (blue). (d) Invariant manifolds $W^U(S_7)$ (violet) and $W^S(S_7)$ (blue). (e) Basins for $b = -0.802$. (f) For the same values of the parameters as in figure (e), the invariant manifolds $W^U(S_7)$ (violet) and $W^S(S_7)$ (blue) are represented.

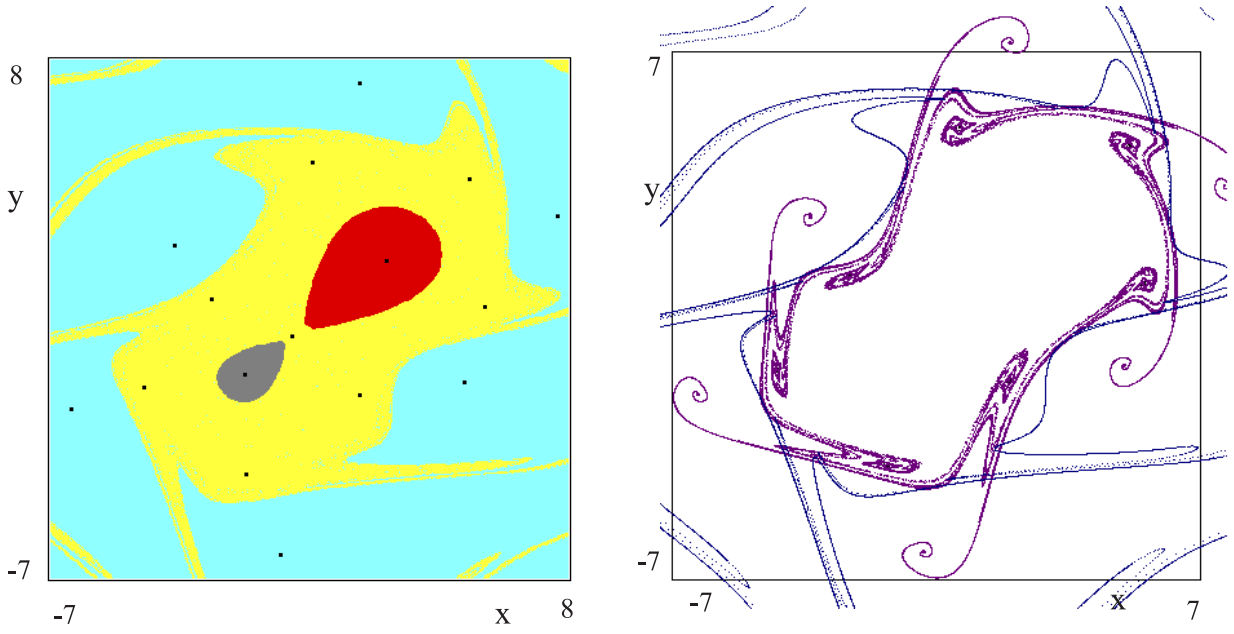

(e) (f)

Fig. 28. (*Continued*)

Fig. 30(b), where homoclinic points of S_6 are still visible. Instead, no homoclinic points of the saddle S_7 exist, $W^U(S_7) \cap W^S(S_7) = \emptyset$, as can be seen in Fig. 30(c).

However, as suggested by Fig. 30(c), a further decrease of b causes the second homoclinic tangency of the manifolds $W_1^U(S_6)$ and $W_1^S(S_6)$, after which the closed curve, saddle-focus connection between

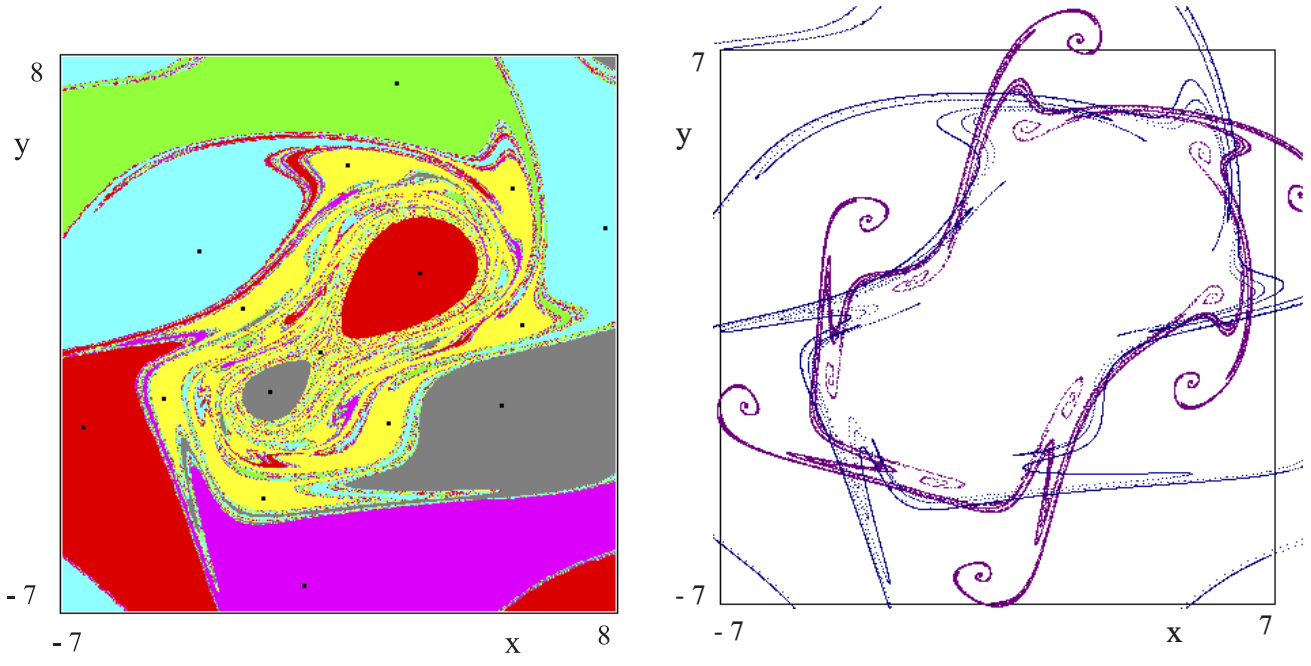

(a) (b)

Fig. 29. (a) $b = -0.81$, the basin of C_7 is the yellow region, and six different colors are used for the basins of $C_{6,i}$. (b) For the same set of parameters, the stable set $W^S(S_6)$ and the unstable set $W^U(S_6)$ are represented by blue and violet, respectively. (c) For the same set of parameters $W^S(S_7)$ and $W^U(S_7)$ are shown in blue and violet, respectively.

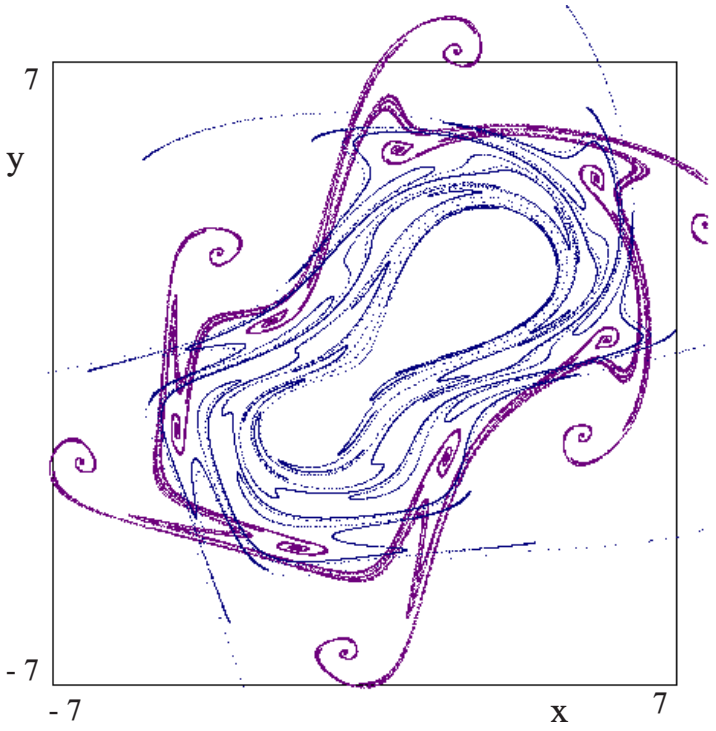

(c)

Fig. 29. (*Continued*)

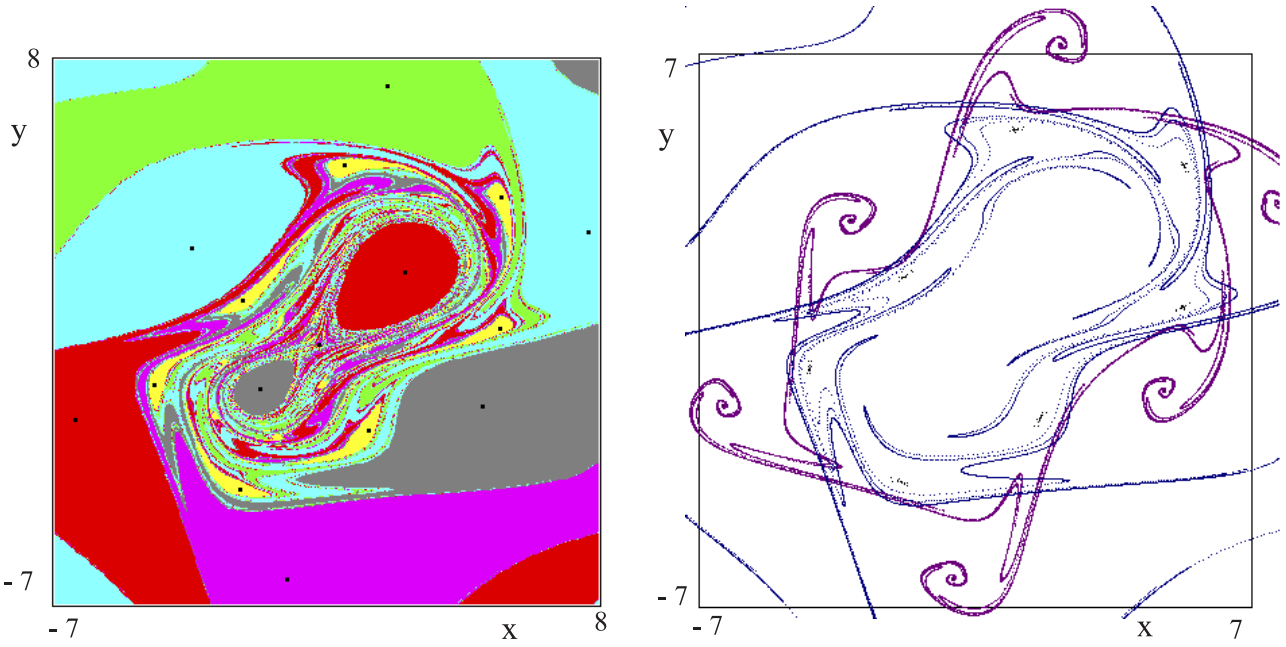

(a) (b)

Fig. 30. $b = -0.82$, the basin of C_7 is the yellow region, and six different colors are used for the basins of $C_{6,i}$. (b) For the same set of parameters, the stable set $W^S(S_6)$ and the unstable set $W^U(S_6)$ are represented by blue and violet, respectively. (c) For the same set of parameters $W^S(S_7)$ and $W^U(S_7)$ are shown in blue and violet, respectively.

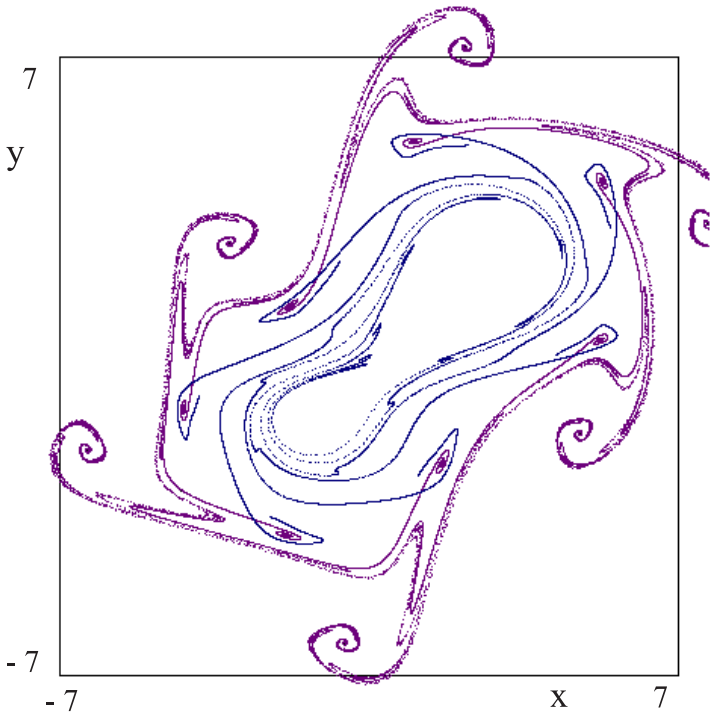

(c)

Fig. 30. (*Continued*)

C_6 and S_6, will appear (for example, it exists at $b = -0.823$), and all the basins of attraction have smooth boundaries.

5. A Family of Polynomial Maps

In order to show that the bifurcations described in Sec. 2 and in the examples of Secs. 3 and 4 are not related to some peculiarity of the maps defined by an S-shaped function, in this section we shall briefly consider the following two-dimensional polynomial map:

$$T: \begin{cases} x' = ax + y \\ y' = bx + cy + dy^3 \end{cases} \tag{7}$$

We fix the values of the parameters $a = 0.2$, $c = 2.1$, $d = -1$, and the parameter b is let to decrease below -0.5. The origin O is a fixed point, whose stability triangle in the (c, b) parameter plane is similar to the one shown in Fig. 7(a), and a supercritical Neimark bifurcation occurs as well as a supercritical pitchfork bifurcation, giving rise to two fixed points, say Q_1 and Q_2. Like in the case of map (1), this family of polynomial maps is symmetric with respect to the origin. However the bifurcations shown in this section are not related to this symmetry property (indeed, they can be observed also in the asymmetric maps obtained from (7) by adding the term, pxy to the second component).

As in the previous examples, we start from a value of b in which the two fixed points Q_1 and Q_2 are stable and the stable set of the saddle O separates their basins of attraction. This is shown in Fig. 31(a), using gray and red colors for the two basins $B(Q_1)$ and $B(Q_2)$ respectively. In this figure we can also see a dark blue region which is the set of points having divergent trajectories, that is, the basin of infinity, and its basin boundary includes the stable set of some saddle cycle. As Fig. 31(b) shows, as b is decreased the two basins $B(Q_i)$ exhibit more and more convolutions around the origin, leading to the creation of closed invariant curves, as shown in Fig. 31(c). In this figure, besides the attracting curve Γ (whose basin is yellow), and the repelling curve $\tilde{\Gamma}$, which is the limit set of the basins $B(Q_i)$, we can also see that the stable set of the origin shrinks towards O, and then an homoclinic tangle will occur. Indeed, the enlargement in Fig. 31(d) clearly shows that the stable and unstable sets of O intersect each other, and we are inside the homoclinic tangle. After the second tangency the homoclinic points disappear leaving two closed invariant

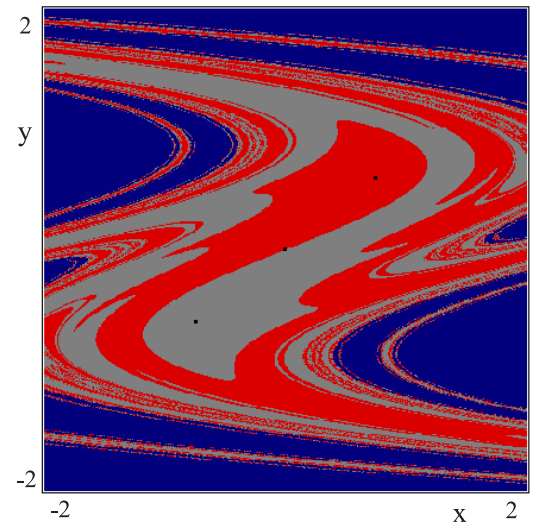

(a)

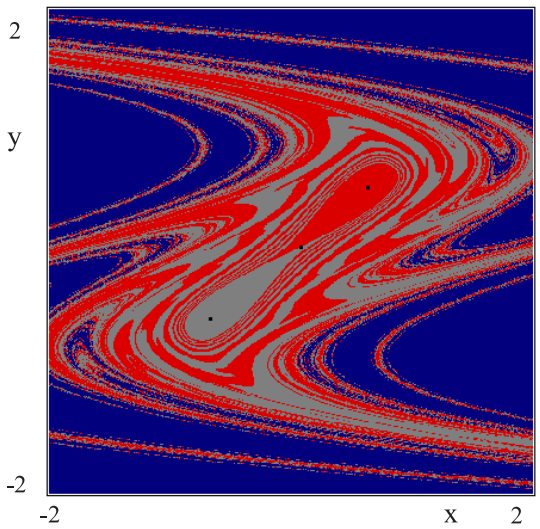

(b)

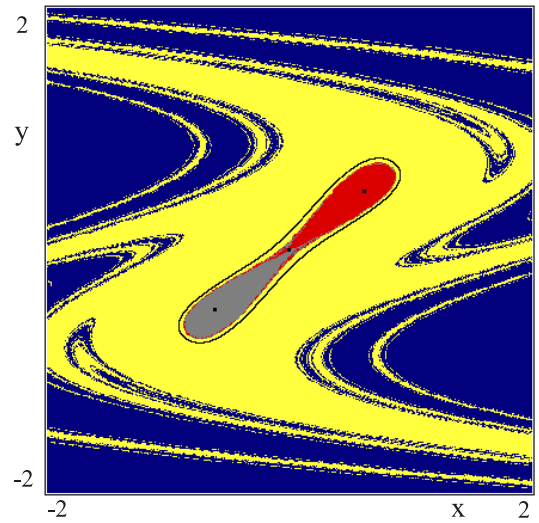

(c)

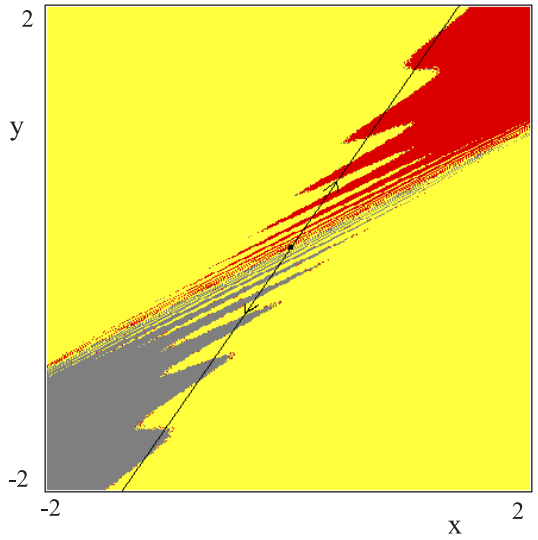

(d)

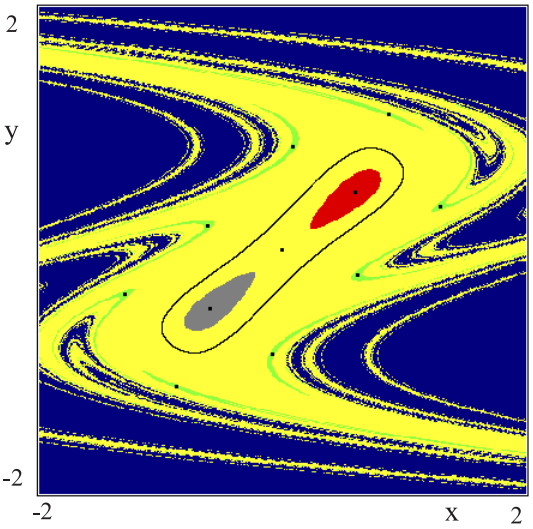

(e)

Fig. 31. Polynomial map (7) with parameters $a = 0.2$, $c = 2.1$, $d = -1$. (a) For $b = -0.6$ the basins of the stable fixed points Q_1 and Q_2 are represented by the gray and red regions, respectively, whereas the dark blue region represents the basin of infinity. (b) $b = -0.685$. (c) $b = -0.69$, besides the two stable fixed points Q_1 and Q_2 an attracting closed curve Γ exists, whose basin is yellow. (d) $b = -0.6934$, enlargement of a neighborhood of the saddle fixed point O, the black line is the unstable set $W^U(O)$, the boundary between the yellow, red and gray regions is given by the stable set $W^S(O)$. (e) $b = 0.7$, after the second tangency two closed invariant repelling curves exist, that form the boundaries of the basins $B(Q_i)$, together with a closed attracting curve, whose basin is represented by the yellow region, and a stable 8-cycle, whose basin is green.

repelling curves which are the boundaries of the basins $B(Q_i)$, shown in Fig. 31(e). In Fig. 31(e) the yellow region denotes the basin of the attracting curve Γ while the green points represent the basin of attraction of an 8-cycle born by a saddle-node bifurcation.

In this family of maps, different from the previous ones, we are not trying to show the details of the bifurcation mechanisms leading to the dynamic situations described above, however, we believe that they are similar to those observed in Secs. 3 and 4, and qualitatively described in Sec. 2, even if they occur in a very narrow interval of values of the parameter b.

Acknowledgments

This work has been performed within the activity of the national research project "Nonlinear models in economics and finance: complex dynamics, disequilibrium, strategic interactions," MIUR, Italy.

References

Agliari, A., Gardini, L. & Puu, T. [2003] "Global bifurcations in Duopoly when the Cournot point is destabilized via a subcritical Neimark bifurcation," *Int. Game Th. Rev.*, in press.

Aronson, D. G., Chory, M. A., Hall, G. R. & McGehee, R. P. [1982] "Bifurcations from an invariant circle for two-parameter families of maps of the plane: A computer assisted study," *Commun. Math. Phys.* **83**, 303–354.

Bai-Lin, H. [1989] *Elementary Symbolic Dynamics* (World Scientific, Singapore).

Birkhoff, G. D. & Smith, P. [1928] "Structure analysis of surface transformations," *J. de Math.* **S9**, 345–379.

Bischi, G. I., Dieci, R., Rodano, G. & Saltari, E. [2001] "Multiple attractors and global bifurcations in a Kaldor-type business cycle model," *J. Evolut. Econ.* **11**, 527–554.

Bischi, G. I., Gallegati, M., Gardini, L., Leonbruni, R. & Palestrini, A. [2003] "Herding behaviours and nonfundamental high frequency asset price fluctuations in financial markets," *Macroecon. Dyn.*, in press.

Dieci, R., Bischi, G. I. & Gardini, L. [2001] "Multistability and role of nonivertibility in a discrete-time business cycle model," *Central European J. Operat. Res.* **9**, 71–96.

Frouzakis, C. E., Adomaitis, R. A. & Kevrekidis, I. G. [1991] "Resonance phenomena in an adaptively-controlled system," *Int. J. Bifurcation and Chaos* **1**, 83–106.

Frouzakis, C. E., Gardini, L., Kevrekidis, I. G., Millerioux, G. & Mira, C. [1997] "On some properties of invariant sets of two-dimensional noninvertible maps," *Int. J. Bifurcation and Chaos* **7**, 1167–1194.

Gardini, L. [1994] "Homoclinic bifurcations in n-dimensional endomorphisms, due to expanding periodic points," *Nonlin. Anal.* **23**, 1039–1089.

Gavrilov, N. K. & Shilnikov, L. P. [1972a] "On three dimensional dynamical systems close to systems with structurally unstable homoclinic curve I," *Mat. USSR Sbornik* **17**, 467–485.

Gavrilov, N. K. & Shilnikov, L. P. [1972b] "On three dimensional dynamical systems close to systems with structurally unstable homoclinic curve II," *Mat. USSR Sbornik* **19**, 139–156.

Gicquel, N. [1996] "Bifurcation structure in a transmission system modelled by a two-dimensional endomorphisms," *Int. J. Bifurcation and Chaos* **8**, 1463–1480.

Guckenheimer, J. & Holmes, P. [1985] *Nonlinear Oscillations, Dynamical Systems, and Bifurcations of Vector Fields* (Springer-Verlag, NY).

Gumowski, I. & Mira, C. [1980] *Dynamique Chaotique* (Cepadues Editions, Toulouse).

Herrmann, R. [1985] "Stability and chaos in a Kaldor-type model," Working Paper DP22, Department of Economics, University of Gottingen.

Kuznetsov, Y. A. [1998] *Elements of Applied Bifurcation Theory*, 2nd edition (Springer-Verlag, NY).

Lorenz, H.-W. [1992] "Multiple attractors, complex basin boundaries, and transient motion in deterministic economic systems," in *Dynamic Economic Models and Optimal Control*, ed. Feichtinger, G. (Elsevier).

Maistrenko, Y. L., Maistrenko, V. L., Vikul, S. I. & Chua, L. [1995] "Bifurcations of attracting cycles from time-delayed Chua's circuit," *Int. J. Bifurcation and Chaos* **5**, 653–671.

Maistrenko, Y. L., Maistrenko, V. L. & Mosekilde, E. [2003] "Torus breakdown in noninvertible maps," *Phys. Rev.* **E67**, 1–6.

Medio, A. & Lines, M. [2001] *Nonlinear Dynamics* (Cambridge University Press, UK).

Mira, C. [1987] *Chaotic Dynamics. From the One-dimensional Endomorphism to the Two-dimensional Diffeomorphism* (World Scientific, Singapore).

Mira, C., Gardini, L., Barugola, A. & Cathala, J. C. [1996] *Chaotic Dynamics in Two-dimensional Noninvertible Maps* (World Scientific, Singapore).

Sushko, I., Puu, T. & Gardini, L. [2003] "The Hicksian floor-roof model for two regions linked by interregional trade," *Chaos Solit. Fract.* **18**, 593–612.

Wiggins, S. [1988] *Global Bifurcations and Chaos, Analytical Methods* (Springer-Verlag, NY).